



UNIVERSIDADE ESTADUAL DE CAMPINAS
Faculdade de Engenharia Elétrica e de Computação

Ricardo Coelho Ferreira

**Massive MIMO Systems Aided By Large Reflecting
Surfaces as a Novelty For 6G Technologies**

**Sistemas MIMO Auxiliados Por Grandes
Superfícies Refletoras Como Novidade Para
Tecnologias 6G**

Campinas

2021

Ricardo Coelho Ferreira

**Massive MIMO Systems Aided by Large
Reflecting Surfaces as a Novelty For 6G
Technologies**

**Sistemas MIMO Auxiliados Por Grandes
Superfícies Refletoras Como Novidade Para
Tecnologias 6G**

Dissertation presented to the School of Electrical and Computer Engineering of the University of Campinas in partial fulfillment of the requirements for the degree of Master in Electrical Engineering, in the area of Telecommunications and Telematics.

Dissertação apresentada à Faculdade de Engenharia Elétrica e de Computação da Universidade Estadual de Campinas como parte dos requisitos exigidos para a obtenção do título de Mestre em Engenharia Elétrica, na área de Telecomunicações e Telemática.

Orientador: Prof. Dr. Gustavo Fraidenraich

Este trabalho corresponde à versão final da dissertação defendida pelo aluno Ricardo Coelho Ferreira, orientada pelo Prof. Dr. Gustavo Fraidenraich.

Campinas

2021

Ficha catalográfica
Universidade Estadual de Campinas
Biblioteca da Área de Engenharia e Arquitetura
Rose Meire da Silva - CRB 8/5974

F413m Ferreira, Ricardo Coelho, 1995-
Massive MIMO systems aided by large reflecting surfaces as a novelty for
6G technologies / Ricardo Coelho Ferreira. – Campinas, SP : [s.n.], 2021.

Orientador: Gustavo Fraidenraich.
Dissertação (mestrado) – Universidade Estadual de Campinas, Faculdade
de Engenharia Elétrica e de Computação.

1. Rádio - Transmissores e transmissão - Desvanecimento. 2. Sistema de
comunicação sem fio. 3. Sistemas de comunicação móvel. 4. Sistemas MIMO.
5. Probabilidade de erro (Matemática). I. Fraidenraich, Gustavo, 1975-. II.
Universidade Estadual de Campinas. Faculdade de Engenharia Elétrica e de
Computação. III. Título.

Informações para Biblioteca Digital

Título em outro idioma: Sistemas MIMO auxiliados por grandes superfícies refletoras
como novidade para tecnologias 6G

Palavras-chave em inglês:

Radio - Transmitters and transmission - Fading

Wireless communication system

Mobile communication systems

MIMO systems

Probability of error (mathematics)

Área de concentração: Telecomunicações e Telemática

Titulação: Mestre em Engenharia Elétrica

Banca examinadora:

Gustavo Fraidenraich [Orientador]

Paulo Cardieri

Sarah Negreiros de Carvalho Leite

Data de defesa: 22-02-2021

Programa de Pós-Graduação: Engenharia Elétrica

Identificação e informações acadêmicas do(a) aluno(a)

- ORCID do autor: <https://orcid.org/0000-0002-9309-1735>

- Currículo Lattes do autor: <http://lattes.cnpq.br/2208884075896775>

COMISSÃO JULGADORA – DISSERTAÇÃO DE MESTRADO

Candidato: Ricardo Coelho Ferreira RA: 228003

Data da defesa: 22 de Fevereiro de 2021

Thesis Title: Massive MIMO Systems Aided by Large Reflecting Surfaces as a Novelty For 6G Technologies

Título da Tese: Sistemas MIMO Auxiliados Por Grandes Superfícies Refletoras Como Novidade Para Tecnologias 6G.

Prof. Dr. Gustavo Fraidenraich(Presidente).

Prof. Dr. Paulo Cardieri.

Profa. Dra. Sarah Negreiros de Carvalho Leite.

A Ata de Defesa, com as respectivas assinaturas dos membros da Comissão Julgadora, encontra-se no SIGA (Sistema de Fluxo de Dissertação/Tese) e na Secretaria de Pós-Graduação da Faculdade de Engenharia Elétrica e de Computação.

Acknowledgements

First of all, I like to thank my parents and sisters that welcomed me all these years for believing in the importance of studies throughout my formation, making it possible for me to reach this stage.

This work would not have been possible without the support of my advisor Dr. Gustavo Fraidenraich partly for the corrections and help with complex deductions but also for the patience in guiding and the opportunity to be part of research groups and projects that certainly helped a lot in my academic formation, I express my gratitude here.

I am grateful to Michelle S. P. Facina, Felipe A. P. De Figueiredo and Eduardo Rodrigues De Lima who contributed a lot for the publication of the results presented here and that made possible the conclusion of this research.

I would like to mention some friends who have accompanied me since the beginning of this journey and who made the experience of the master's program more pleasant by living together, among them Monikelli Wippel, Letícia Sathler, and Lucas Cunha, Iuri Monteiro, Leandro Jordão and Guilherme Vetorazzi, among many others that I was fortunate to know and share moments Wilher Oliveira, Gabriela Domingues, Paulo César, Gustavo Tejerina.

This study was financed in part by the Coordenação de Aperfeiçoamento de Pessoal de Nível Superior - Brasil (CAPES) - Finance Code 001.

“Heard joke once: Man goes to doctor. Says he’s depressed. Says life seems harsh and cruel. Says he feels all alone in a threatening world where what lies ahead is vague and uncertain. Doctor says, "Treatment is simple. Great clown Pagliacci is in town tonight. Go and see him. That should pick you up." Man bursts into tears. Says, "But doctor...I am Pagliacci.”

Alan Moore, **Watchmen**

Abstract

Large intelligent surfaces (LIS) is a promising technology for the sixth generation (6G) of mobile communications due to its potential to improve the signal to noise ratio (SNR), increase spectral efficiency, and even make it possible to reduce energy consumption in the radio base station (BS) during transmission. The LIS is a panel formed by cells that can reflect electromagnetic waves to make beamforming and cancel the channel phase, the surface is formed by metamaterials that can change the phase of the incident waves with a quantized angle that can be controlled digitally by software allowing that the signal resulting from the sum of all components reflected by the LIS has a phase adapted to nullify the effect of the channel phase. The channel information is estimated by machine learning algorithms and more efficient phase estimations implies better phase adjustments at the LIS, but due to the system's non-idealities, we have a residual phase error that in this work is modeled by the Von Mises distribution. We divided our study into two chapters, the first referring to systems with a single antenna at the BS considering the existence of a straight and unobstructed line for electromagnetic wave propagation *a.k.a.* line of sight (LoS) with Nakagami- m fading and we ignore the possibility of a direct link between the user, in the second part we consider an antenna array at the base station and including a direct link between the user and the BS but neglecting the LoS by considering Rayleigh fading channels. For the single antenna BS scenario, we derive the *exact* bit error probability considering quadrature amplitude modulation (M -QAM) and binary phase-shift keying (BPSK) when the number of LIS elements, n , is equal to 2 and 3 considering that the channel fading coefficients are Nakagami- m . Also, based on the central limit theorem (CLT), and considering a large number of reflecting elements, we present an accurate approximation and upper bounds for the bit error rate. Through several Monte Carlo simulations, we demonstrate that all derived expressions perfectly match the simulated results. In the antenna array scenario, we consider Rayleigh flat fading for each subchannel between the BS, the LIS, and the user and we apply a precoder at the base station to have the maximum ratio transmission (MRT). Based on the CLT, we conclude that the overall channel has an equivalent Gamma fading whose parameters are derived from the moments of the channel fading between the

antenna array and LIS, and also from the LIS to the single user. Assuming that the equivalent channel can be modeled as a Gamma distribution, we propose very accurate closed-form expressions for the bit error probability and a very tight upper bound. For the case where the LIS is not able to perform perfect phase cancellation, that is, under phase errors, it is possible to analyze the system performance considering the analytical approximations and the simulated results obtained using the well known Monte Carlo method. The analytical expressions for the parameters of the Gamma distribution are very difficult to be obtained due to the complexity of the nonlinear transformations of random variables with non-zero mean and correlated terms. Even with perfect phase cancellation, all the fading coefficients are complex due to the link between the user and the base station that is not neglected in this study.

Resumo

Large Intelligent Surfaces (LIS) é uma tecnologia promissora para a sexta geração (6G) de comunicações móveis devido ao seu potencial para melhorar a relação sinal-ruído (SNR), aumentar a eficiência espectral e ainda possibilitar a redução do consumo de energia na estação rádio base (BS) durante a transmissão. O LIS é um painel formado por células que podem refletir ondas eletromagnéticas para fazer beamforming e remover a fase do canal, a superfície é formada por metamateriais que podem alterar a fase das ondas incidentes com um ângulo quantizado que pode ser controlado digitalmente por software permitindo que o sinal resultante da soma de todas as componentes refletidas pelo LIS possua uma fase adaptada para cancelar o efeito da fase do canal. Esta fase é estimada por algoritmos de aprendizado de máquina e quanto mais eficiente a estimativa melhor será o processo de ajuste de fase, mas devido às não idealidades do sistema, temos um erro de fase residual que neste trabalho é modelado pela distribuição de Von Mises. Dividimos nosso estudo em dois capítulos, o primeiro referindo-se a sistemas com apenas uma antena na BS, considerando a presença de uma linha direta de propagação de ondas eletromagnéticas *a.k.a.* line of sight (LoS) com desvanecimento Nakagami- m e nós ignoramos a possibilidade de um link direto com o usuário, já na segunda parte consideramos um arranjo de antenas na estação base e incluindo um link direto entre o usuário e a BS, mas negligenciando a LoS ao considerar canais com desvanecimento Rayleigh. Para o cenário da BS de uma antena, derivamos a probabilidade de erro de bit exata considerando modulação M -QAM e BPSK quando o número de elementos do LIS, n , é igual a 2 e 3 considerando que os coeficientes de desvanecimento do canal são Nakagami- m e o LIS tem um erro de fase com distribuição de Von Mises. Além disso, com base no teorema do limite central, e considerando um grande número de elementos refletores, apresentamos uma aproximação precisa e limites superiores para a taxa de erro de bit. Por meio de várias simulações de Monte Carlo, demonstramos que todas as expressões derivadas correspondem perfeitamente aos resultados simulados.

No cenário de matriz de antenas, consideramos o Rayleigh flat fading para cada subcanal entre a BS, o LIS e o usuário e aplicamos um precoder na estação base para ter a transmissão de razão máxima (MRT). Com base no teorema do limite central (CLT), concluímos que o canal total tem um desvanecimento Gamma equivalente cujos parâmetros

são derivados dos momentos estatísticos do canal entre o arranjo de antenas e LIS, e também do LIS para o usuário. Assumindo que o canal equivalente pode ser modelado como uma distribuição Gama, propomos expressões de forma fechada muito precisas para a probabilidade de erro de bit e um limite superior muito restrito. Para o caso em que o LIS não é capaz de realizar o cancelamento de fase perfeito, ou seja, sob erros de fase, é possível analisar o desempenho do sistema considerando as aproximações analíticas e os resultados simulados obtidos pelo método de Monte Carlo. As expressões analíticas para os parâmetros da distribuição Gama são muito difíceis de serem obtidas devido à complexidade das transformações não lineares de variáveis aleatórias com média diferente de zero e termos correlatos. Mesmo com o cancelamento de fase perfeito, todos os coeficientes de desvanecimento são complexos devido à ligação entre o usuário e a estação base que não é negligenciada neste estudo.

Publications

This study produced two articles published in scientific journals.

1. **Large Intelligent Surfaces Communicating Through Massive MIMO Rayleigh Fading Channels**; Ricardo Coelho Ferreira, Michelle S. P. Facina, Felipe A. P. de Figueiredo, Gustavo Fraidenraich, Eduardo Rodrigues de Lima; DOI: 10.3390/s20226679, MDPI Sensors, 22 November 2020 [1].
2. **Bit error probability for large intelligent surfaces under double-nakagami fading channels**; Ricardo Coelho Ferreira, Michelle S. P. Facina, Felipe A. P. de Figueiredo, Gustavo Fraidenraich, Eduardo Rodrigues de Lima; DOI: 10.1109/OJCOMS.2020.2996797, IEEE Open Journal of the Communications Society; under Creative Commons License; Volume: 1, 25 May 2020 [2].

List of Notation

A	Matrix or tensor (capital bold)
a	Vector (bold)
$\text{var}(X)$	Variance
$\text{cov}(X)$	Covariance
$E[\cdot]$	Expected value
$Q(\cdot)$	Gaussian error function
$\mathbf{X}^H = (\mathbf{X}^*)^T$	Hermitian adjoint (transpose conjugate)
$\mathbf{A} \circ \mathbf{B}$	Hadamard tensor product
$I_p(\cdot)$	Modified Bessel function of first kind and order p
$\varphi_p = E[e^{jpX}]$	Moment generating function
$\alpha_p = \text{Re}\{\varphi_p\}$	Cosine trigonometric moment
$\beta_p = \text{Im}\{\varphi_p\}$	Sine trigonometric moment

Summary

List of Notation

1	Introduction	15
2	Error probability for BPSK systems with Large Intelligent Surfaces communicating through double-Nakagami Fading channels	24
2.1	Large reflecting surfaces, a brief introduction	24
2.2	System Model	24
2.3	Fading Distribution	27
2.4	Bit Error Probability	30
2.5	Numerical Results	32
3	Large Intelligent Surfaces Communicating Through Massive MIMO Rayleigh Fading Channels	37
3.1	System Model	37
3.2	Von Mises Distributed Continuous Phase Estimation Errors	39
3.3	Approximated Gamma Fading Distribution	40
3.4	Error Probability Calculations	41
3.5	Simulated Results	43
4	Conclusion	48
5	Appendix	49
5.1	Error probability for BPSK systems with Large Intelligent Surfaces communicating through double-Nakagami Fading channels	49
5.2	Large Intelligent Surfaces Communicating Through Massive MIMO Rayleigh Fading Channels	52
5.3	Mean and Variance of the Overall Channel Fading Coefficient with Von Mises Distributed Phase Errors	58

5.4 Trigonometric Moments of a Von Mises Random Variable	66
References	68

1 Introduction

The future of mobile digital communications in the age of the internet of things (IoT) requires to optimize the energy consumption for transmission, improve the signal to noise ratio (SNR) at the receiver, increase the spectral efficiency, and propose communication protocols, channel estimation methods and beamforming strategies suitable for the adopted system model.

Many solutions have been proposed as alternatives to the sixth generation of mobile communications. Zhang et al. [3] make an excellent review of the literature on these emerging techniques, citing among them large intelligent surfaces (LIS), holographic beamforming (HBF), angular orbital momentum (OAM) multiplexing, laser and visible-light communications (VLC) [4] and the advent of quantum computing which is increasingly present in large technology companies like Google and allows unmatched performance and security for quantum communication systems. Nawaz et al. [5] investigate the use of quantum machine learning strategies to improve the performance of the processes involved in the network structure since we mess with many parallel operations involving large arrays and tensors with data loaded and that through quantum computing can be mapped into large tensors product spaces where operations are handled by quantum processors that take advantage of the phenomenon of quantum superposition to achieve large communication rate and encryption security.

The demand for data rate has increased exponentially in the last years, mainly due to the emergence of new services such as the internet of things (IoT) and the video on demand. Sensors, objects, and everyday items can communicate, generate, exchange, and consume data with minimal or no human intervention. One of the solutions to support this new increasing data rate relies on solutions such as antenna arrays and electromagnetic mirrors. However, they can be expensive and present high power consumption at the transmitter [6].

Since then, there are already some variants of this technology [7]. Intelligent reflecting surfaces (IRS) are composed of reflecting elements capable of changing the incident signal in frequency, amplitude, or polarization [8]. Large intelligent meta-surfaces (LIM) are reconfigurable

surfaces composed of projected meta-materials that can change the incident signals based on their physical properties[9]. On the other hand, software-defined surfaces (SDS) are capable of being configured by software solutions [10]. Passive intelligent surfaces (PIS) reflect the incident signals without applying any power gain to the reflected signal[11].

As an attempt to deal with this design compromise between increasing spectral efficiency and minimizing transmission power consumption, several methods involving large intelligent surfaces (LIS) have been proposed. A LIS, which is an array composed of a massive number of low-cost reflecting elements, is capable of reflecting the incident signals with adjustable phase-shifts [12]. As they leverage ultra-reliability, high spectral, and power efficiency of the digital communication systems, LIS-equipped systems meet the requirements posed by various emerging application scenarios such as the industrial IoT [13].

The proposal to make use of large intelligent surfaces to improve transmission quality in massive MIMO systems is recent and has been gaining visibility in the literature as a concrete solution for the sixth generation (6G) of mobile communications and has presented a competitive performance in comparison with classic methods like relaying switches. A concept, similar to LIS, was first mentioned in 2015 at the University of California Berkeley project [14]. The general idea consists of wallpapers that are electromagnetically active and have built-in processing power. There is a compact integration of large numbers of tiny antennas with reconfigurable processing networks.

One of the great challenges for the implementation of the LIS is to estimate the channel and obtain the distribution of the fading coefficients. Wang et al. [15] propose channel estimation methods for multiuser massive MIMO systems assisted by LIS and present alternatives to decrease the training time necessary to have complete knowledge of the channel coefficients. Tataria et al. [16] discuss practical aspects of real-time implementation of LIS, especially in terms of processing and applications in radio frequency (RF) communications. Elbir et al. [17] present a deep learning framework for channel estimation, considering the massive MIMO scenario using mm-Wave.

Yu et al. [18] propose the use of LIS to improve the coverage of a cellular IoT in the so-

called beyond fifth-generation (B5G). The LIS project aims to minimize the energy consumption and study the impact of channel parameters on spectral efficiency.

The work of Hum et al. [19], for example, proposes a solution very similar to LIS technology. It discusses, from a theoretical point of view, the future challenges and the possibility of using array lenses, micro-electro-mechanical systems (MEMS), and reconfigurable reflect-arrays to make electronic beamforming by changing the polarization, amplifying signals and increasing the signal to noise ratio. The use of reflecting surfaces to perform beamforming has emerged in the last three years as an alternative to the sixth generation of mobile communications. Hu et al. [20] use adjacent surfaces, covered with a magnetic and active material capable of being electronically and intelligently manipulated, to solve wireless communication tasks [21].

LIS technology can be divided into two types, passive and active. Although both of them can constructively combine the signals, minimizing the noise effect, there are fundamental differences. The LIS with passive elements can only reflect the incident signals, modifying their phases without any reflection amplitude control. On the other hand, active LIS achieves better signal to noise ratio due to reflection amplitude control. It is necessary to perform power allocation at the reflectors, which requires high computational complexity [22].

Despite recent proposals in the literature to tackle all these challenges [23], achieving the optimal power allocation for active LIS beamforming is a complex optimization problem for itself. The search for the precoder vector and the design of the matrix with phase-shifts involves the optimization of non-convex functions, which is an intricate task [24].

Regarding the phase adjustments common to the two types of LIS, they are designed for two reasons. To cancel the channel phase, improving the SNR or even destructively at the non-intended receiver to avoid interference and enhance security/privacy. According to [25], the LIS can control and optimize the refraction and reflection towards anomalous directions, thus altering the spatial distribution of the intended and interfering signals. But, it is worth mentioning that this process is susceptible to phase errors.

According to Zhang [26] the matrix of reflectors operates by controlling diodes on each LIS element alternating between the states on and off to control the bias voltage. Since the

diodes are digitally controlled, there is a limited amount of bits to represent the reflection angles. Therefore the phase is quantized, and there are random phase errors.

Considering that such errors do not exist, the framework investigated in [22, 27] takes into account a LIS composed of passive antenna elements with reconfigurable characteristics. They do not require any dedicated energy source for either decoding, channel estimation, or transmission. The authors came across some non-convex problems that are solved through the use of optimization techniques. Based on majorization-maximization alternated by fractional programming, it is possible to optimize energy efficiency.

Taha et al. [28] propose a training process based on deep learning. Using a massive number of passive reflectors and a small number of active ones, the LIS can learn the channel parameters and autonomously optimize the data transmission.

Following this idea, Basar et al. [8] present closed-form solutions for optimization problems. Parameters related to LIS design, power allocation, precoder, and phase shift matrix are derived and influence the performance of the system directly.

Besides, LIS can also be useful in smart radio environments employing millimeter-wave band (frequencies around 30-100 GHz). In the absence of line of sight (LoS) paths, systems operating at such bands cannot work correctly due to the high attenuation caused by the absorption of atmospheric gases. Then, LIS-equipped systems can create LoS paths connecting the base station to devices [29]. These and other advantages are evident in [30], in which the authors present a comparative performance study between classic relaying and reflecting surfaces at high-frequency bands when there is no LoS path.

Yang et al. [31] proposed a transmission protocol for a system that combines LIS and orthogonal frequency division multiplexing (OFDM) with channel estimation, the reflectors were divided into clusters, and the adopted methodology considers that adjacent reflectors share the same reflection coefficient. Only the channel resulting from the combination of the clusters needs to be estimated.

Ye et al. [32] propose techniques to minimize the symbol error rate (SER) by optimizing the phase shifts and the precoder for a MIMO reconfigurable intelligent surface (RIS) considering

a finite alphabet of symbols. Among the strategies proposed are to fix the phase shifts and obtain the optimal precoder or to fix the precoder and find the phase shifts, that solution is useful to reduce the dimensionality of the optimization task and also the performance of the proposed RIS strategy is compared with a relay system and we see the advantage of using the techniques proposed by the authors.

Wu et al. [33] develop a mmWave point-to-point communication system assisted by multiple intelligent subsurfaces with passive reflecting elements, and antenna arrays on the transmitter and receiver. The authors derived the system achievable rate and have found the optimal precoding and power allocation for the LIS phase shift design. He et al. [34] investigate the theoretical limits and Cramér-Rao bounds for the LIS performance in a MIMO 5G system dealing with mmWave and considering the existence of a direct path (NLoS and LoS).

Dardari [35] derives analytical expressions for the channel gain and the spatial degrees-of-freedom (DoF) for the optimal LIS design considering MIMO systems. The analysis is based on electromagnetic theory and employs only geometric arguments. Jung et al. [36] consider that a MIMO system assisted by LIS can be modeled as an LoS after phase cancellation. The authors also analyze the theoretical limitations of the practical system's performance considering spatially correlated Rician channels and demonstrate that the NLoS component can be neglected when the number of antennas increases.

Yan et al. [37] present a multiuser MIMO (Mu-MIMO) system in which intelligent electromagnetic reflectors perform passive beamforming. The authors also propose to design a receiver with two estimation modules. One for the signal transmitted by the base station and the other, to estimate the additional On/Off information associated with the reflectors that modulate the digital signal arriving at them.

Badiu et al. [38] shows that the perfect estimation of the reflection angles at the LIS array is unfeasible, so we have to model the phase errors due to the estimation and discretization errors. The authors claim that the overall channel, including the LIS, can be modeled as Nakagami- m distributed, for phase errors having a generic distribution.

Cavers [39] defines maximal ratio transmission (MRT), establishing that the base station

applies a vector of complex weights to compensate the downlink channel by canceling the phase and perform a signal reinforcement. He also shows a generalization for the effects of fading when the system has multiple users, although there is no exact generic solution for the optimal precoder in this scenario.

Makarfi et al. [40] propose to apply reconfigurable intelligent surfaces to expand coverage and improve the signal-to-noise ratio of a vehicular network, which can be seen as a case study of the IoT area using this new massive MIMO solution. The authors explore the idea of using smart radio environments for IoT problems and discuss some relevant aspects beyond 5G to establish communication between vehicles.

Qian et al. [41] present a MIMO system that uses LIS and has an array of antennas on the transmitter and receiver. The signals suffer uncorrelated Rayleigh fading in each channel. The authors obtain good approximations and performance studies based on analytical derivations of the statistical moments associated with the largest eigenvalues of the Wishart matrices related to the LoS and NLoS component. Without losing generality, they assume that the largest eigenvalues have a Gamma distribution and their moments are a function of the number of LIS elements and the number of antennas in the array.

Björnson et al. [42] discuss how the correlation matrix of the LIS elements can be computed under certain conditions, considering Rayleigh fading channels with a direct path between the signal and the final user. In this study, the authors make a more geometric analysis of the problem considering a rectangular panel formed by several reflectors and their constructive parameters, thereby establishing a relationship between the degrees of freedom of the LIS and the rank of the autocorrelation matrix of the reflector panel. Asymptotic analyzes of the SNR variation and channel hardening are also performed when the number of antennas and reflectors increase.

Note that the phase estimation errors is modeled as zero mean Von Mises distribution [38], which has a concentration parameter, κ , that helps us model the accuracy of the estimation. Large values of the Von Mises κ implies small errors, when $\kappa \rightarrow \infty$ the zero mean Von Mises probability density function is impulsive at zero, and for $\kappa = 0$ the probability distribution is the

uniform distribution.

Analytically obtaining the equivalent fading distribution and the bit error probability is quite intricate due to the considerable sums and transformations of random variables with distinct distributions.

Some authors have employed a similar approach to the one used here, but most of them adopt restrictive models. In [43], the authors have used the central limit theorem (CLT) to obtain an approximate probability distribution and calculate the outage probability in scenarios involving many reflectors and only one antenna at the base station. The authors only consider a phase error with uniform distribution (worst case of phase estimation) and a channel subjected to the Rayleigh fading. They do not provide any expression for a small number of reflectors.

In most previous research, it is assumed that the channel fading is Rayleigh distributed. Of course, the Rayleigh-fading model is known to be a reasonable assumption for the fading encountered in many wireless communications systems. However, many measurement campaigns [44, 45] show that the Nakagami- m distribution provides a much better fitting for the fading channel distribution. Since the Nakagami- m distribution has one more free parameter, it allows for more flexibility. It moreover contains the Rayleigh distribution ($m = 1$), the one-sided Gaussian distribution ($m \rightarrow 0.5$), and the uniform distribution on the unit circle¹ ($m \rightarrow 1$) as special (extreme) cases. The Nakagami- m distribution is a general, but an approximate solution to the random phase problem [46]. The exact solution involves the knowledge of the distribution and the correlations of all of the partial waves composing the total signal. It becomes infeasible due to its complexity. This has been circumvented by Nakagami [46], who, through empirical methods based on field measurements followed by a curve-fitting process, obtained the approximate distribution.

In the first part of this study, we consider passive elements and focus on the bit error rate. Our main contribution is the derivation of *exact* expressions for the BPSK and M -QAM bit error probability for an arbitrary number of reflectors n . The expressions derived here allow us to predict how the channel parameters and the phase error distribution impact the performance of the communication between the base station and the end-user. One of the main problems solved

here is true of a very general statistical application that can be used in countless applications. In particular, we find an exact solution to the problem of obtaining the distribution of the sum of random vectors whose amplitudes follow the product of two Nakagami- m distributions and whose phases follow the Von Mises distribution. Note that the literature solves this problem but for a very limited scenario, namely vectors with fixed amplitudes and uniform phases. Certainly, our solution is much more general than this. Of course, in both cases, as the number of vectors increases the CLT can be used. But, for an arbitrary finite number of vectors, our solution is much more general.

In the second part of the study, we investigate the performance of a system employing LIS, also known as large reflective surfaces (LRS), taking into account Rayleigh channels and phase errors due to imperfect channel phase cancellation. This work is very general since it considers a direct link between the base station with multiple antennas and the single user. We investigate the system performance and quality of the proposed approximations for channel distribution in terms of the Kullback-Leibler divergence metric. We also present analytical expressions for the bit error probability and very tight upper bounds for different scenarios in terms of the Von Mises parameter.

This study is divided into two papers [2], [1] trying to cover some gaps in the literature, with regard to obtaining analytical solutions in the form of simple algebraic expressions involving the channel parameters and the Von Mises parameter for the single antenna transmitter in Nakagami- m fading channels scenario and for the antenna array transmitter in Rayleigh fading scenario, in this way we were able to simplify the analysis of a very generalist system model that may include the direct link with the user, may have one or more antennas at the base station and we maintain the validity of the analysis even when the phase correction algorithm is not efficient. Badiu et al. [38] use the central limit theorem to solve a simpler scenario with one Rayleigh NLoS channel and a Rician LoS channel, but considering a single antenna transmitter. Björnson et al. [42] propose asymptotic approaches in a scenario that takes into account the correlation of the LIS elements but is also restricted to the context with a single antenna transmitter which simplifies the analytical solutions.

The remainder of this study is organized as follows, in the second chapter we talk about

the single transmitter case, where the Rayleigh fading environment includes channels between the single user, single transmitter, and several reflector panels between them. The second chapter considers multiple transmitters sending the same symbol and a Nakagami- m fading channel between the LIS and the user and transmitters. The sections present the system model, the fading distribution of each subchannel, we model the LIS phase correction errors and present the overall fading distributions and the bit error probability. Several calculations are left for the appendix to simplify the reading.

2 Error probability for BPSK systems with Large Intelligent Surfaces communicating through double-Nakagami Fading channels

2.1 Large reflecting surfaces, a brief introduction

According to Gong et al. [47], the LIS is an array composed of two-dimensional scattering (near to zero thickness) cells, these cells can be metallic or dielectric metasurfaces with some electromagnetic properties, that depend on the design parameters and allows us to control the phase of the reflected signals. The reflected and diffracted electromagnetic waves follow the Fresnel equations and Snell's law and the special arrangement of the LIS cells causes a shift of the resonance frequency and thus a change of boundary conditions, this mechanism causes the phase changes.

There are digitally controlled chips inside the structure of the metasurface of each cell, and each one of them interacts with a scattering element communicating with a controller programmed by software. The tuning of the controller allows us to design the LIS according to the needs, giving great versatility to this technology.

2.2 System Model

As shown in Fig. 3.1, we consider a single-input single-output (SISO) system formed by a base station (BS) with a single antenna sending signals to LIS. The array is composed of n reflector elements, in which the incident signals are reflected with a calculated phase-shift. Only a single-antenna user is considered.

The system is composed of two channels. The single-input multiple-output (SIMO) channel between BS and LIS is modeled by the fading coefficient $H_{1k} \in \mathbb{C}^{1 \times n}$. The multiple-input single-output (MISO) channel between LIS and the user is modeled by the coefficient

$H_{2k} \in \mathbb{C}^{n \times 1}$. Both of them are independent random variables modelled by the Nakagami- m distribution.

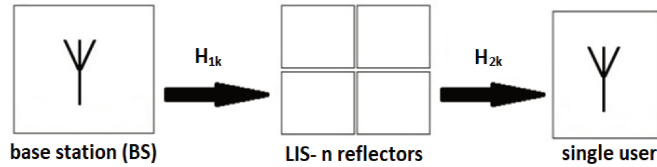


Figure 2.1: System model.

Let X be the transmitted symbol with zero mean and unit variance. According to Badiu et al. [48], the incident signal on the single-antenna user can be expressed as

$$Y = \sqrt{\gamma_0} \sum_{k=1}^n e^{j\phi_k} H_{1k} H_{2k} X + W, \quad (2.1)$$

in which ϕ_k is the phase adjustment performed by the LIS, W is the additive noise and follows a Gaussian distribution, $W \sim \mathcal{N}(0, \sigma_W^2)$, γ_0 is the average signal to noise ratio for a single reflector, $|H_{1k}|$ and $|H_{2k}|$ for $\forall k$ are Nakagami- m distributed with the following probability density function

$$f_{|H_{ik}|}(x) = \frac{2m^m}{\Gamma(m)\Omega^m} x^{2m-1} e^{-\frac{m}{\Omega}x^2}, \quad (2.2)$$

in which m is the shape parameter and Ω is the spread parameter, and $|\cdot|$ denotes the absolute value.

We can assume that the phase introduced by the product of the two complex fading coefficients, H_{1k} and H_{2k} are almost entirely cancelled by LIS. But there are remaining errors due to the quantization bit limitation, estimation of the channel phases, and synchronism error. The total residual phase error can be modeled as a Von Mises random variable θ_k . The zero-mean Von Mises distribution has real support in the range from $-\pi$ to π , and the κ parameter describes how scattered the probability density function is from the mean.

The Von Mises distribution is a continuous probability distribution on a circle analogous to the Gaussian distribution but with the entire non-zero part of the PDF distributed in a range of size 2π centered on the mean. This distribution was previously used to simulate the azimuth angles [10] and model the phase error [48] in LIS-based systems. It is versatile to represent

random angles since the concentration parameter is related to the distribution variance and models how closely the angle is from the mean.

Let θ_k be the phase error modeled by a Von Mises random variable Θ and concentration parameter κ , In other words, $\Theta \sim \text{Von Mises}(\kappa)$. The Von Mises distribution has the following PDF [49]

$$f_{\Theta}(\theta) = \frac{1}{2\pi I_0(\kappa)} e^{\kappa \cos(\theta)}, \quad (2.3)$$

in which $I_0(\kappa)$ is the modified Bessel function of first kind and order 0. The parameter κ indicates the spread of the distribution. Large κ means that the phase error is concentrated in a small interval. When $\kappa = 0$, the phase errors are equally probable and follow the uniform distribution.

Consider that $\theta_{H_{1k}} = \arg(H_{1k})$ is the phase of the channel between BS and the LIS elements and $\theta_{H_{2k}} = \arg(H_{2k})$ is the phase of the link between each LIS element and the user. The LIS attempts to perform phase cancellation with respect to the composite channel $H_{1k}H_{2k}$, by rotating the incident signal by a phase shift ϕ_k , in such a way that $\theta_{H_{1k}} + \theta_{H_{2k}} + \phi_k = 0$. In practice, the phase correction is not perfect and residual errors are left, that is

$$\theta_k = \phi_k + \theta_{H_{1k}} + \theta_{H_{2k}}. \quad (2.4)$$

Isolating the variable ϕ_k in (2.4) and substituting in (2.1), we have that

$$\begin{aligned} Y &= \sqrt{\gamma_0} \sum_{k=1}^n e^{j\phi_k} H_{1k} H_{2k} X + W = \sqrt{\gamma_0} \sum_{k=1}^n e^{j\theta_k} e^{-j(\theta_{H_{1k}} + \theta_{H_{2k}})} H_{1k} H_{2k} X + W \\ &= \sqrt{\gamma_0} \sum_{k=1}^n e^{j\theta_k} e^{-j(\theta_{H_{1k}} + \theta_{H_{2k}})} |H_{1k}| |H_{2k}| \times e^{j(\theta_{H_{1k}} + \theta_{H_{2k}})} X + W \\ &= \sqrt{\gamma_0} \sum_{k=1}^n e^{j\theta_k} |H_{1k}| |H_{2k}| X + W. \end{aligned} \quad (2.5)$$

We can define the composite fading coefficient H as

$$H = \frac{1}{n} \sum_{k=1}^n e^{j\theta_k} |H_{1k}| |H_{2k}|, \quad (2.6)$$

and therefore, the output at the receiver (2.5) can be written as

$$Y = n\sqrt{\gamma_0} H X + W, \quad (2.7)$$

The distribution of H , given in (2.6), is of fundamental importance to our problem. Since we have sum of terms $|H_{1k}| |H_{2k}|$, we have to derive the distribution of the product of two Nakagami- m distribution. Fortunately, from [46], we know that the distribution of $Z = |H_{1k}| |H_{2k}|$, is given by

$$f_Z(z) = \frac{4z^{m_1+m_2-1} K_{m_1-m_2} \left(2z \prod_{i=1}^2 \sqrt{\frac{m_i}{\Omega_i}} \right)}{\prod_{i=1}^2 \Gamma(m_i) \left(\frac{\Omega_i}{m_i} \right)^{\frac{m_2+m_1}{2}}}, \quad (2.8)$$

in which $\Gamma(\cdot)$ represents the Gamma function, Z is a random variable with Double-Nakagami distribution, while m_i and Ω_i are the parameters of each Nakagami- m coefficient.

It is important to highlight that the phase distribution of the complex fading coefficients is not relevant in our analysis, but only the magnitude.

2.3 Fading Distribution

In this section, we derive the distributions of $|H|$ using the channel parameters and the characteristic function associated with the random phase error for $n = 2$ and $n = 3$. Moreover, it is also proposed an approximate distribution for large values of n .

It is possible to rewrite (2.6) as $H = \frac{1}{n} \sum_{k=1}^n |H_{12k}| e^{j\theta_k}$, in which $|H_{12k}| = |H_{1k}| |H_{2k}|$ is the magnitude of the combined fading coefficients. The squared fading coefficient magnitude can be written as:

$$|H|^2 = \left(\sum_{k=1}^n R_k \cos \theta_k \right)^2 + \left(\sum_{k=1}^n R_k \sin \theta_k \right)^2, \quad (2.9)$$

in which $R_k = \frac{1}{n} |H_{12k}|$, $\theta_1 \dots \theta_n$ are independent Von Mises random variables. R_k is the k -th sample direction, and the resultant direction is $|H|$. Note that (2.9) can be written as

$$|H|^2 = C^2 + S^2, \quad (2.10)$$

in which C and S are the in-phase and quadrature components given by

$$C = \sum_{k=1}^n R_k \cos \theta_k, \quad (2.11)$$

and

$$S = \sum_{k=1}^n R_k \sin \theta_k. \quad (2.12)$$

2.3.1 Exact Distribution of $|H|$ for $n = 2$ and $n = 3$

The general solution to the computation problem of $R = \left| \sum_{i=1}^n R_i e^{j\theta_i} \right|$, *i.e.*, the magnitude of a linear combination of complex variables with constant magnitudes and random phases uniformly distributed, was obtained by Maghsoodi [50]. However, our problem requires that R_1, R_2, \dots, R_n be random variables, so we need to remove the conditioning (considering that the magnitudes are given) and apply the law of total probability to obtain the complete solution. Therefore, in order to apply this result to our problem, we multiply the solution given in [50] by the distribution of the product of two Nakagami- m distributions, *i.e.*, the double-Nakagami distribution given in (2.8). Then, we perform the integration with respect to the variables R_1, R_2, \dots, R_n .

The *exact* PDF of $|H|$ for $n = 2$ and $n = 3$ is given by (2.13) and (2.14), respectively. The symbol $U(\cdot)$ denotes the Heaviside unit step function, and $\bar{r}_2(\phi) = \sqrt{r_1^2 + r_2^2 + 2r_1r_2 \cos \phi}$.

$$f_{|H|}(r) = \frac{2}{\pi} \int_0^\infty \int_0^\infty \frac{U(4r_1^2 r_2^2 - (r^2 - r_1^2 - r_2^2)^2)}{\sqrt{4r_1^2 r_2^2 - (r^2 - r_1^2 - r_2^2)^2}} \cdots \\ \times \prod_{k=1}^2 \left(\frac{4r_k^{m_1+m_2-1} K_{m_1-m_2} \left(2r_k \sqrt{\frac{m_1 m_2}{\Omega_1 \Omega_2}} \right)}{\Gamma\left(\frac{m_1}{\Omega_1}\right)^{\frac{m_1+m_2}{2}} \Gamma\left(\frac{m_2}{\Omega_2}\right)^{\frac{m_1+m_2}{2}}} \right) dr_k, \quad n = 2. \quad (2.13)$$

$$f_{|H|}(r) = \frac{2}{\pi^2} \int_0^\pi \int_0^\infty \int_0^\infty \int_0^\infty \frac{U(4r_3^2 \bar{r}_2(\phi)^2 - (r^2 - \bar{r}_2(\phi)^2 - r_3^2)^2)}{\sqrt{4r_3^2 \bar{r}_2(\phi)^2 - (r^2 - \bar{r}_2(\phi)^2 - r_3^2)^2}} \cdots \\ \times \prod_{k=1}^3 \left(\frac{4r_k^{m_1+m_2-1} K_{m_1-m_2} \left(2r_k \sqrt{\frac{m_1 m_2}{\Omega_1 \Omega_2}} \right)}{\Gamma\left(\frac{m_1}{\Omega_1}\right)^{\frac{m_1+m_2}{2}} \Gamma\left(\frac{m_2}{\Omega_2}\right)^{\frac{m_1+m_2}{2}}} \right) d\phi, \quad n = 3. \quad (2.14)$$

Fig. 2.1 shows a comparison between the exact and simulated PDF for $m = 1, 2, 3$. As can be seen, as the value of m increases, the mean of the distribution also increases, that is, the larger the m parameter, the better the condition of the channel.

2.3.2 Approximated Distribution of $|H|$ For Large n

Unfortunately, the exact distribution for large n is very intricate and its evaluation becomes computationally prohibitive. However, as n increases, the distributions of C and S ,

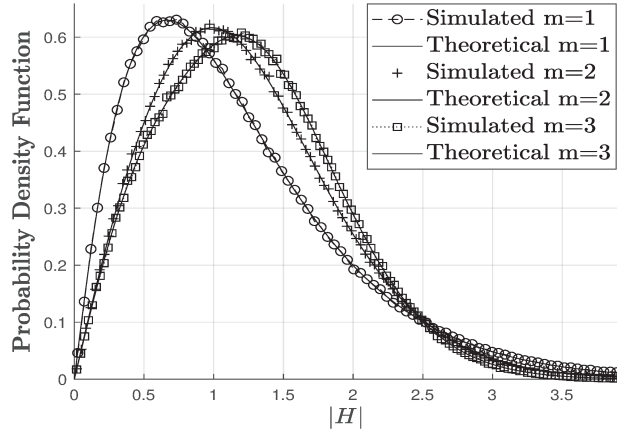


Figure 2.1: Exact PDF of $|H|$ for $n = 2$ double-Nakagami.

given in (2.11) and (2.12) respectively, become approximately Gaussian due to central limit theorem [51], that is $C \sim \mathcal{N}(\mu_C, \sigma_C^2)$, and $S \sim \mathcal{N}(\mu_S, \sigma_S^2)$. Since C and S are uncorrelated (see Appendix C), for the Gaussian case, this condition implies that they are also independent random variables [52], and therefore their joint distribution can be given as

$$f_{C,S}(x, y) = \frac{1}{2\pi\sigma_C\sigma_S} e^{-\frac{(x-\mu_C)^2}{2\sigma_C^2}} e^{-\frac{(y-\mu_S)^2}{2\sigma_S^2}}. \quad (2.15)$$

The analytical expression for the mean μ_C and variance σ_C^2 of C , are expressed by (5.1) and (5.10), respectively in Appendix 5.2. In the same way, the mean μ_S and variance σ_S^2 of S are given by (5.11) and (5.16), respectively in Appendix 5.1.2.

Since we are interested in the distribution of the fading envelope, that is $\rho = |H|$, we can perform a change of variables as $x = \rho \cos \phi$ and $y = \rho \sin \phi$, and then $f_{P,\Phi}(\rho, \phi) = \rho f_{C,S}(x, y)$ can be written as

$$f_{P,\Phi}(\rho, \phi) = \frac{\rho}{2\pi\sigma_C\sigma_S} e^{-\frac{(\rho \cos(\phi) - \mu_C)^2}{2\sigma_C^2}} e^{-\frac{(\rho \sin(\phi) - \mu_S)^2}{2\sigma_S^2}}. \quad (2.16)$$

Uniformly Distributed Phase Error

Considering that the phase error is uniformly distributed, the mean and variance of C and S can be further simplified. Assume $\kappa = 0$ and θ_k is a zero mean random variable, therefore according to (5.1) and (5.11), the mean of C is given by

$$\mu_C = \mu_1\mu_2 E[\cos \theta_k] = \mu_1\mu_2\alpha_1 = 0, \quad (2.17)$$

in which $E[\cdot]$ is the expected value of a random variable and α_p is the real part for the characteristic function φ_p that can be defined as

$$\varphi_p = E[e^{jp\theta}] = \alpha_p + j\beta_p. \quad (2.18)$$

Note that $\beta_p = 0$, because the imaginary part of the characteristic function is associated with a sine function, which is an odd function and the PDF is symmetrical. Then, φ_p is a real number and can be given as $\varphi_p = \alpha_p = \frac{I_p(\kappa)}{I_0(\kappa)}$.

The mean of S is given by

$$\mu_S = \mu_1\mu_2 E[\sin \theta_k] = \mu_1\mu_2\beta_1 = 0. \quad (2.19)$$

Using (5.10) and (5.16), the variance of C and S can be calculated as

$$\sigma_C^2 = \sigma_S^2 = \frac{\sigma_{12}^2 + \mu_1\mu_2}{2n}. \quad (2.20)$$

For these values of mean and variance, (2.16) simplifies to

$$f_{P,\Phi}^U(\rho, \phi) = \frac{\rho}{2\pi\sigma_C^2} e^{-\frac{\rho^2}{2\sigma_C^2}}. \quad (2.21)$$

2.4 Bit Error Probability

The bit error probability for the M -QAM and BPSK modulations can be found according to [53, 54] respectively as

$$P_e^{QAM}(\bar{\gamma}) = 1 - \left(1 - 2 \left(1 - \frac{1}{\sqrt{M}} \right) Q \left[\sqrt{\frac{3\bar{\gamma} \log_2 M}{(M-1)}} \right] \right)^2, \quad (2.22)$$

and

$$P_e^{BPSK}(\bar{\gamma}) = Q(\sqrt{\bar{\gamma}}), \quad (2.23)$$

in which $Q(\cdot)$ is the Gaussian error function, $\bar{\gamma} = \frac{E_b}{2\sigma_W^2}$, E_b is the energy per bit, and M is the number of symbols.

Under multipath propagation, the mean probability of error can be written as

$$\bar{P}_e^{QAM}(\bar{\gamma}) = \int_0^\infty P_e^{QAM}(n^2\bar{\gamma}r^2) f_{|H|}(r) dr, \quad (2.24)$$

$$\bar{P}_e^{BPSK}(\bar{\gamma}) = \int_0^\infty P_e^{BPSK}(n^2\bar{\gamma}r^2) f_{|H|}(r) dr, \quad (2.25)$$

in which $f_{|H|}(r)$ is given by (2.13) and (2.14) for $n = 2$ and $n = 3$, respectively.

When n is large and from some assumptions, we can derive elegant expressions for the bit error probability as follows.

2.4.1 Bit Error Probability for Large n

Considering that C and S are Gaussian distributed, then the error probability can be calculated as

$$\bar{P}_e^{QAM}(\bar{\gamma}) = \int_{-\pi}^{\pi} \int_0^\infty P_e^{QAM}(n^2\bar{\gamma}\rho^2) f_{P,\Phi}(\rho, \phi) d\rho d\phi. \quad (2.26)$$

The same way, the bit error probability for BPSK can be written as

$$\bar{P}_e^{BPSK}(\bar{\gamma}) = \int_{-\pi}^{\pi} \int_0^\infty P_e^{BPSK}(n^2\bar{\gamma}\rho^2) f_{P,\Phi}(\rho, \phi) d\rho d\phi. \quad (2.27)$$

Considering the Chernoff bound $Q(x) \leq \frac{1}{2}e^{-\frac{1}{2}x^2}$, then the upper bound of the error probability can be calculated by (2.28) on the next page. Here, $k_1 = M + 3\gamma \log_2(M)n^2\sigma_S^2 - 1$, $k_2 = M + 6\gamma \log_2(M)n^2\sigma_S^2 - 1$, and $\sigma_{min} = \min(\sigma_C, \sigma_S)$.

$$\begin{aligned} \bar{P}_e^{QAM}(\bar{\gamma}) \leq & - \left(k_1 (\sqrt{M} - 1) e^{\frac{(M-1)(\mu_C^2 + \mu_S^2)}{2k_2\sigma_{min}^2}} - 2k_2\sqrt{M} e^{\frac{(M-1)(\mu_C^2 + \mu_S^2)}{2k_1\sigma_{min}^2}} \right) \dots \\ & \times \frac{(\sqrt{M} - 1)^2 (\sqrt{M} + 1) e^{-\frac{\mu_C^2 + \mu_S^2}{2\sigma_{min}^2}}}{k_1 k_2 M} \end{aligned} \quad (2.28)$$

Following the same reasoning in (2.27), and defining $\sigma_{min} = \min(\sigma_C, \sigma_S)$, we obtain an upper bound for the BPSK modulation as

$$\bar{P}_e^{BPSK}(\bar{\gamma}) \leq \frac{e^{-\frac{\gamma n^2(\mu_C^2 + \mu_S^2)}{2\gamma n^2\sigma_{min}^2 + 1}}}{2(2\gamma n^2\sigma_{min}^2 + 1)}. \quad (2.29)$$

2.4.2 Uniform Phase Distribution

The worst case for the phase error is the uniform distribution, in which all angles are equally likely. Considering BPSK modulation, the bit error probability can be written as

$$\bar{P}_e^{BPSK}(\bar{\gamma}) = 2\pi \int_0^\infty P_e^{BPSK}(n^2\bar{\gamma}\rho^2) f_{P,\Phi}^U(\rho, \phi) d\rho, \quad (2.30)$$

where $f_{P,\Phi}^U(\rho, \phi)$ is defined in (2.21). Its closed-form resembles the channel under Rayleigh fading presented in [53]. For the sake of clarity, it is repeated here as

$$\bar{P}_e^{BPSK}(\bar{\gamma}) = \frac{1}{2} \left(1 - \frac{n\sqrt{\bar{\gamma}}}{\sqrt{n^2\bar{\gamma} + \frac{1}{\sigma_C^2}}} \right). \quad (2.31)$$

For the general M -QAM modulation, the error probability considering uniform phase error is given as

$$\bar{P}_e^{QAM}(\bar{\gamma}) = 2\pi \int_0^\infty P_e^{QAM}(n^2\bar{\gamma}r^2) f_{P,\Phi}^U(\rho, \phi) d\rho. \quad (2.32)$$

Unfortunately, there is no closed-form solution to (2.32). However, we can neglect the terms $Q(\cdot)^2$ and then obtain an approximation for the M -QAM bit error probability as

$$\bar{P}_e^{QAM}(\bar{\gamma}) \approx \frac{2 \left(\sqrt{M} - 1 \right) \sigma_C^2 \left(\sqrt{\frac{(M-1) \log(8)}{n^2\bar{\gamma}\sigma_C^2 \log(M)} + 9} - 3 \right)}{\sqrt{M} \sqrt{\frac{(M-1) \log(8)}{n^2\bar{\gamma}\sigma_C^2 \log(M)} + 9}}. \quad (2.33)$$

2.5 Numerical Results

In this section, we present some numerical results to validate the Monte Carlo simulations obtained from 10^6 realizations. For simplicity, the variables σ_1^2 and σ_2^2 assume unitary value.

Fig. 2.1 shows the probability density function of $|H|$ for $\kappa \in \{0, 1, 2\}$ and $n = 128$. We can observe that the simulated curves match very well the approximated results.

Table 2.1 presents the mean squared error (MSE) between the approximate the simulated distributions for different values of n . It is evident that the accuracy of the proposed approach becomes higher as n increases. For example, the error is less than 5% for $n \geq 32$ and practically zero for $n > 128$.

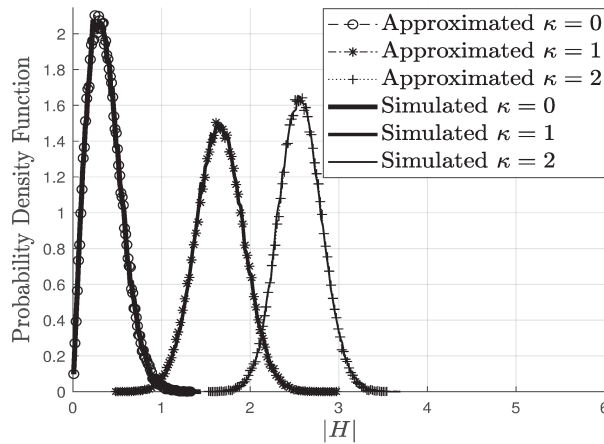


Figure 2.1: PDF of $|H|$ for $n = 128$ and different values of κ .

Table 2.1: Mean Squared Error of the Approximated PDF.

n	Mean Square Error (MSE)	MSE (%)
8	0.1077	10.77
16	0.0784	7.84
32	0.0451	4.51
64	0.0143	1.43
128	0.0001	0.01

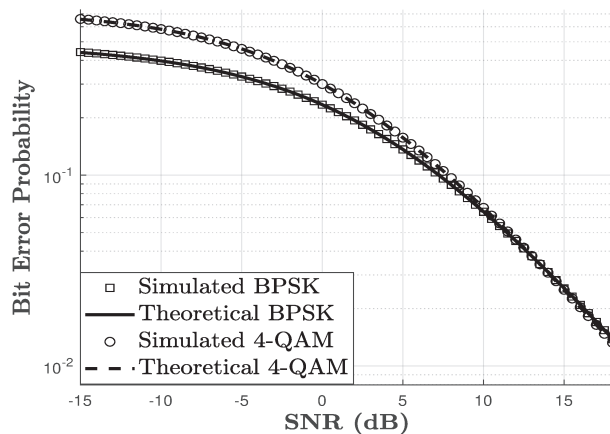


Figure 2.2: Exact bit error probability for $n = 2$.

Considering $n = 2$, Fig. 2.2 shows the exact bit error probability given by (3.15) and (2.25), for 4-QAM and BPSK, respectively. As expected, the theoretical and simulated curves are indistinguishable.

In Fig. 2.3, we present the bit error probability for 4-QAM modulation for $n = 32$ and $n = 128$. As can be seen, the proposed approximated distribution curve is very close to the

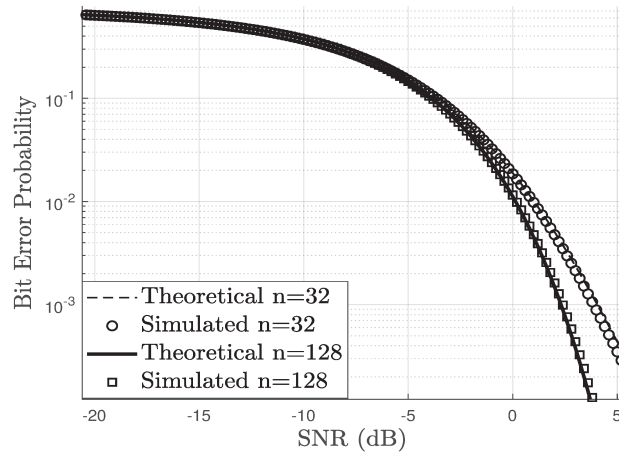


Figure 2.3: Error probability for 4-QAM and different values of reflecting elements, n .

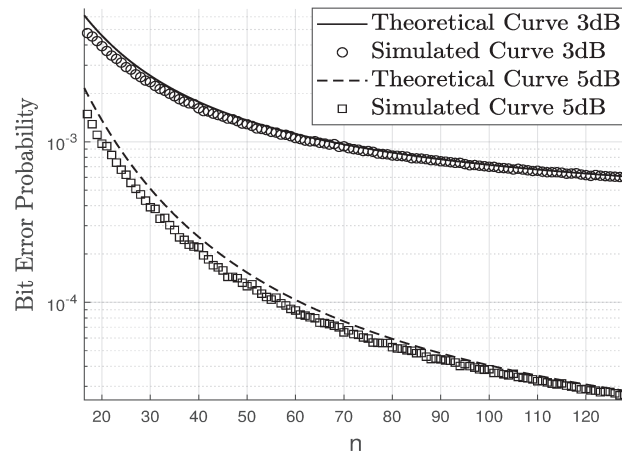


Figure 2.4: Error probability for different values of n .

simulated curve. Its accuracy increases for larger values of n , as predicted by the law of large numbers.

Fig. 2.4 shows the behavior of BER of 4-QAM modulation as a function of the number of reflectors, n , for two values of SNR. As expected, the error decreases as n increases.

Fig. 2.5 shows the theoretical and simulated BER for 4-QAM, $n = 32$ and different values of κ . It is possible to see that BER decreases as κ increases.

Fig 2.6 shows the bit error probability for 4-QAM modulation as a function of the concentration parameter κ for a fixed signal to noise ratio of -25 dB and $n = 256$. Note that as κ increases, the BER decreases fast, since the phase errors are more concentrated around the mean.

In Fig. 2.7, we can verify that the upper bound, proposed in (2.29), for the bit error rate

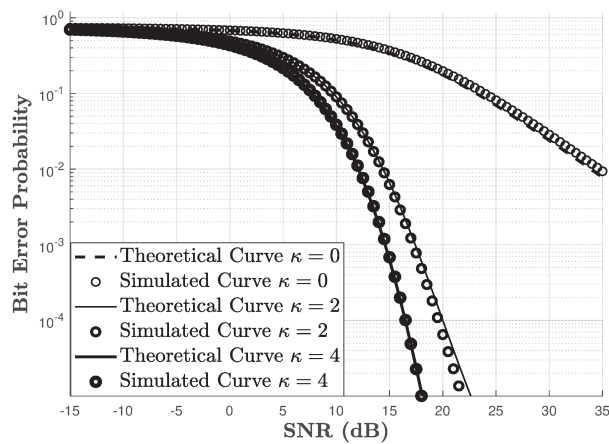


Figure 2.5: Approximate bit error probability for 4-QAM and $n = 32$.

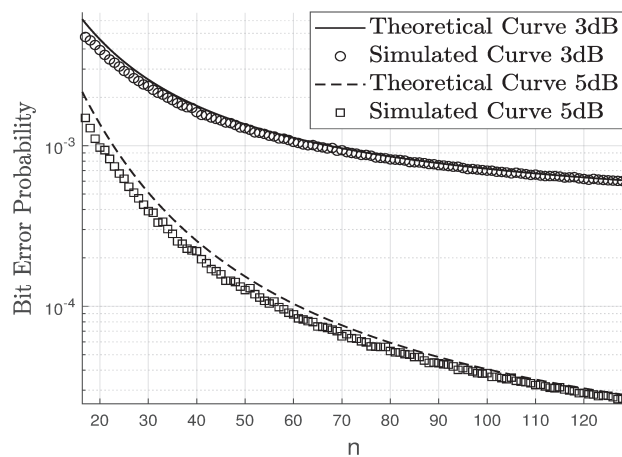


Figure 2.6: Error probability for 4-QAM and different values of κ .

for BPSK modulation and $n = 16$, works correctly and can be useful to approximate the integral formula of (2.27).

Fig. 2.8 shows (2.26) and its approximation proposed in (2.33), considering the 16-QAM modulation with $n = 16$. As can be seen, the approximation is very accurate, especially for large SNR values. Also, we present the result for the upper bound proposed in (2.28). It is possible to see that the upper bound is very tight to the numerical solution.

Finally, Fig. 2.9 shows the bit error probability for different combinations of m_1 and m_2 as a function of the signal to noise ratio. As well known in the literature, for a conventional single input single output channel, the greater the m parameter, the better the performance in terms of BER [55]. It is interesting here to observe that the equivalent parameter m is the product $m_1 m_2$, that is, the greater the product, the better the performance.

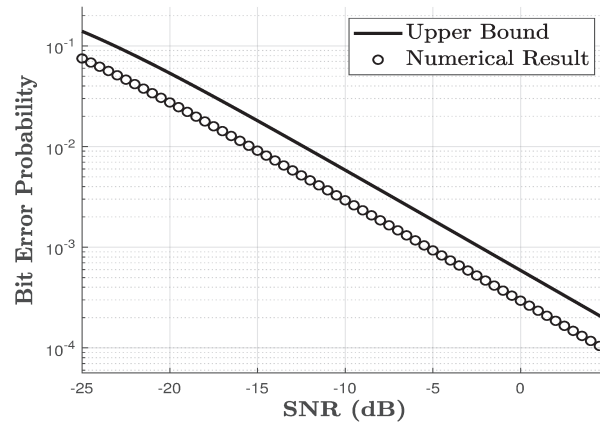


Figure 2.7: Comparison between the BPSK upper bound given in (2.29) and the exact result for $n = 16$.

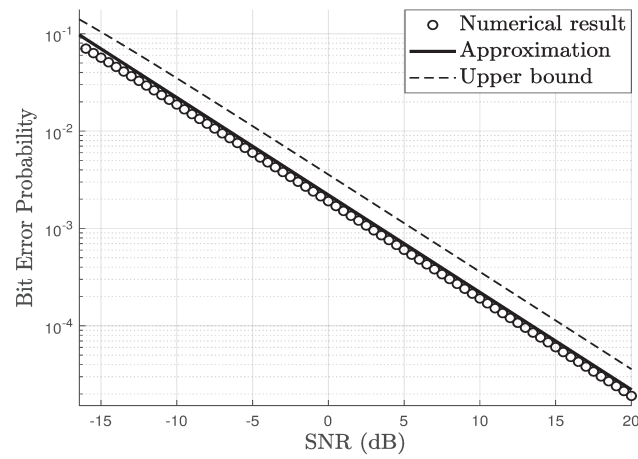


Figure 2.8: Approximate bit error probability and upper bound for $n = 16$ using 16-QAM modulation

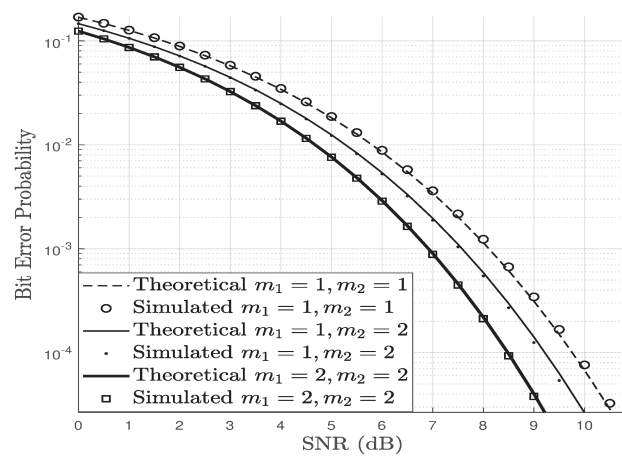


Figure 2.9: Bit error probability for channels with different parameters m_1 and m_2 , assuming 4-QAM modulation, $n = 64$, and $\kappa = 4$.

3 Large Intelligent Surfaces Communicating Through Massive MIMO Rayleigh Fading Channels

3.1 System Model

In this section, we describe the mathematical model adopted in this paper and present the rationale to justify the models used for the channel, the distribution of the fading coefficients in the direct (LoS) and indirect (NLoS) links, in addition to the probability distribution associated with the error of phase accomplished by the LIS when performing the beamforming.

This paper considers a multiple-input single-output (MISO) system between a base station (BS) equipped with an antenna array composed of M antennas and a single-antenna user as shown in Figure 3.1. The signal path passes through the LIS environment dividing the system fading in an LoS component between the BS and the user. There are two indirect paths, between each antenna and the LIS reflector, and between each reflector and the user, these indirect links form a composite channel between the base station and the user. We suppose that the LIS is far from the BS, and the user is also far from the LIS. So, the fading coefficients are modeled as uncorrelated Rayleigh.

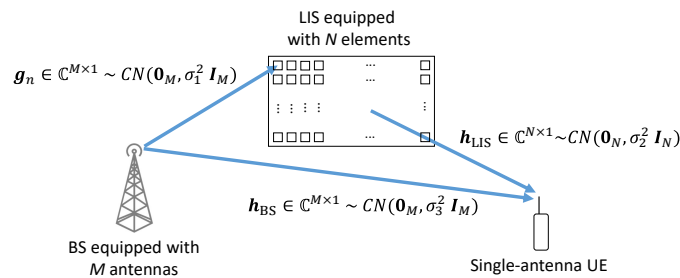


Figure 3.1: System Model.

In this formulation the signal received by the user can be written as

$$y = (\mathbf{h}_{LIS}^H \Phi^H \mathbf{G}^H + \mathbf{h}_{BS}^H) \mathbf{x} + \zeta, \quad (3.1)$$

where $\mathbf{h}_{LIS} \in \mathbb{C}^{N \times 1}$ is the Rayleigh channel between the LIS and the user, $\mathbf{G} = [\mathbf{g}_1 \dots \mathbf{g}_N] \in \mathbb{C}^{M \times N}$ is the Rayleigh channel between the BS and the LIS, $\mathbf{h}_{BS} \in \mathbb{C}^{M \times 1}$ is the complex normal fading of the direct path between the antenna array and the user (LoS component), $\mathbf{x} \in \mathbb{C}^{M \times 1}$ is the transmitted symbol after precoding and $\Phi = \text{diag}([e^{-j\phi_1} \dots e^{-j\phi_N}]) \in \mathbb{C}^{N \times N}$ is a diagonal matrix representing the response of the LIS where $\phi_n \in [0, 2\pi]$, $\forall n$ is the adjustable phase-shift produced by the n th LIS's element. The variable $\zeta \sim \mathcal{CN}(0, 1)$ is the additive white Gaussian noise (AWGN) term. The Tx signal \mathbf{x} is defined as $\mathbf{x} = \mathbf{u}s$ where $\mathbf{u} \in \mathbb{C}^{M \times 1}$ is the precoding vector and $s \sim \mathcal{CN}(0, 1)$ is the data symbol. The precoding vector \mathbf{u} is applied by the antenna array at the BS before the transmission.

Considering the MRT criterion, the optimal precoder is given as [56]

$$\mathbf{u} = \sqrt{p} \frac{\mathbf{w}^H}{\|\mathbf{w}\|} \quad (3.2)$$

where \sqrt{p} is the precoder gain and \mathbf{w} is the overall channel defined as

$$\mathbf{w} = \mathbf{h}_{LIS}^H \Phi^H \mathbf{G}^H + \mathbf{h}_{BS}^H. \quad (3.3)$$

Let η_{ki} and θ_i be the phases of g_{ki} and h_i^{LIS} , respectively. Therefore, we can rewrite each channel fading coefficient as

$$w_k = \sum_{i=1}^N |g_{ki}| |h_i^{LIS}| e^{j(\phi_i - \theta_i - \eta_{ki})} + h_k^{BS} \quad (3.4)$$

From (3.4), we see that the best situation occurs when the composite fading coefficient is perfectly corrected by the LIS and we can state that $\phi_i = \theta_i + \eta_{ki}$. But this scenario is unfeasible because perfect channel state information is not a very realistic assumption. Therefore, both cases are approached: (i) the case where the LIS is able to perform perfect phase cancellation, and; (ii) the case where imperfect cancellation is assumed.

Considering the first case, the composite channel can be written as

$$w_k = \sum_{i=1}^N |g_{ki}| |h_i^{LIS}| + h_k^{BS}. \quad (3.5)$$

Let $C_{BS,k} = \text{Re}\{h_k^{BS}\}$ and $S_{BS,k} = \text{Im}\{h_k^{BS}\}$. Then, the square of the fading vector norm can be written as $\|\mathbf{w}\|^2 = \mathbf{w}^H \mathbf{w}$ and

$$\|\mathbf{w}\|^2 = \sum_{k=1}^M \left[\left(\sum_{i=1}^N |g_{ki}| |h_i^{LIS}| + C_{BS,k} \right)^2 + S_{BS,k}^2 \right]. \quad (3.6)$$

To evaluate the system performance and understand the relationship between the bit error rate and the energy per bit applied by the transmitter, we need to know how the fading coefficients of the overall channel are distributed. Therefore, we need to obtain the statistical moments and the distribution of $\|\mathbf{w}\|^2$.

3.2 Von Mises Distributed Continuous Phase Estimation Errors

Since the phase adjustments performed by the intelligent reflectors are imperfect and cannot completely cancel the channel phase, a term associated with the phase error appears in the equation of the composite channel phase.

Consider that $\phi_i = \theta_k + \eta_{ki} + \delta_{ki}$ is the phase correction performed by the LIS, so the fading coefficients for each antenna is

$$w_k = \sum_{i=1}^N |g_{ki}| |h_i^{LIS}| e^{j\delta_{ki}} + h_k^{BS} \quad (3.7)$$

where the term δ_{ki} is the phase error, here supposed as Von Mises distributed with probability density function

$$f_{\Delta}(\delta) = \frac{1}{2\pi I_0(\kappa)} e^{\kappa \cos \delta}. \quad (3.8)$$

Therefore, we have that

$$\mathbf{w} = (|\mathbf{G}| \circ \mathbf{\Delta}) |\mathbf{h}_{LIS}| + \mathbf{h}_{BS}^H, \quad (3.9)$$

This error model considers a matrix $\mathbf{\Delta} \in \mathbb{C}^{M \times N}$ in which we have the Von Mises phase errors and the Haddamard product is an elementwise product between the phase errors and each channel fading magnitude.

In this case, the moment generating function (MGF) of the Von Mises distribution is useful to obtain the trigonometric moments that are needed to obtain the mean and variance of the

fading coefficients. For a random variable δ Von Mises distributed, the MGF can be calculated by

$$E [e^{jp\delta}] = \alpha_p + j\beta_p, \quad (3.10)$$

where $\alpha_p = \frac{I_p(\kappa)}{I_0(\kappa)}$ and $\beta_p = 0$ are defined in terms of the modified Bessel function of first kind.

3.3 Approximated Gamma Fading Distribution

Since each fading coefficient w_k is the summation of independent and equally probable random variables, we can apply the central limit theorem (CLT). So, for large values of N each w_k is approximately complex Gaussian.

The term $\|\mathbf{w}\|^2$ is the sum of squared Gaussian random variables whose generalized distribution is the Gamma distribution. Let $V \sim \Gamma(\alpha, \beta)$ be a Gamma-distributed variable with shape parameter α and rate parameter β , therefore its probability density function is given as

$$f_V(v; \alpha, \beta) = \frac{\beta^\alpha v^{\alpha-1} e^{-\beta v}}{\Gamma(\alpha)} \quad (3.11)$$

Note that the mean of the Gamma random variable V is given by $E[V] = \frac{\alpha}{\beta}$, and the variance as $\text{var}[V] = \frac{\alpha}{\beta^2}$ [52]. We can compute the mean and variance of $\|\mathbf{w}\|^2$, denoted here as $\mu_{\|\mathbf{w}\|^2}$ and $\sigma_{\|\mathbf{w}\|^2}^2$, respectively, and match with $E[V]$ and $\text{var}[V]$. Using this rationale, the following can be written: $\mu_{\|\mathbf{w}\|^2} = \frac{\alpha}{\beta}$ and $\sigma_{\|\mathbf{w}\|^2}^2 = \frac{\alpha}{\beta^2}$.

Solving this linear equation system, we get that

$$\alpha_{\|\mathbf{w}\|^2} = \frac{\mu_{\|\mathbf{w}\|^2}^2}{\sigma_{\|\mathbf{w}\|^2}^2}, \quad \beta_{\|\mathbf{w}\|^2} = \frac{\mu_{\|\mathbf{w}\|^2}}{\sigma_{\|\mathbf{w}\|^2}^2} \quad (3.12)$$

therefore, with the mean and variance of $\|\mathbf{w}\|^2$, we can generate its Gamma approximated probability density function. Although the idea might seem very simple, the mean and variance of the channel norm are very difficult to be obtained. For the sake of clarity, we detail these calculations in Appendix 5.2, for the case where there are no phase errors. For this case, the mean $\mu_{\|\mathbf{w}\|^2}$ and variance $\sigma_{\|\mathbf{w}\|^2}^2$, are given in (5.39) and (5.67), respectively. In the same way, for the

case where phase error occurs, Appendix 5.3 presents the mean $\mu_{\|\mathbf{w}\|^2}$ and variance $\sigma_{\|\mathbf{w}\|^2}^2$ as in (5.98) and (5.113), respectively.

The trigonometric moments needed to perform the calculations are in the Appendix 5.4.

3.3.1 Kullback–Leibler Divergence

To evaluate the accuracy of approximating $\|\mathbf{w}\|^2$ as a Gamma random variable, we can use Kullback-Leibler divergence [57]. The Gamma distribution will be compared with the simulation obtained by the Monte Carlo method.

Although the distribution of the fading coefficient is continuous, for purposes of numerical calculation, we estimate the PDF with a finite number of points and thus we also sample the Gamma distribution and calculate the Kullback-Leibler divergence in its discrete form [57]

$$D_{KL}(D_1||D_2) = \sum_{x \in \chi} d_1(x) \log \left(\frac{d_1(x)}{d_2(x)} \right), \quad (3.13)$$

where D_1 and D_2 are the simulated and the theoretical distributions, respectively, whose probability distribution functions are $d_1(x)$ and $d_2(x)$ respectively and χ is the set of points available to represent the distributions.

3.4 Error Probability Calculations

The error probability for the M -QAM modulation can be approximately obtained by [53]

$$P_e^{QAM}(\gamma) = 1 - \left(1 - 2 \left(1 - \frac{1}{\sqrt{\mathcal{M}}} \right) Q \left[\sqrt{\frac{3\gamma \log_2 \mathcal{M}}{\mathcal{M} - 1}} \right] \right)^2. \quad (3.14)$$

where \mathcal{M} is the size of the M -QAM constellation. Under Gamma fading, the mean error probability can be calculated as

$$\bar{P}_e^{QAM}(\gamma) = \int_0^{\infty} P_e^{QAM}(\gamma v) f_{\|\mathbf{w}\|^2}(v) dv, \quad (3.15)$$

where $\gamma = p\gamma_0$ and γ_0 is the SNR at the receiver while \bar{P}_e^{QAM} is the mean error probability considering the fading coefficient v and the Gamma pdf $f_{\|\mathbf{w}\|^2}(v)$.

Therefore the error probability can be expressed as

$$\bar{P}_e^{QAM}(\gamma) = \int_0^{\infty} P_e^{QAM}(\gamma v) \frac{\beta^\alpha v^{\alpha-1} e^{-\beta v}}{\Gamma(\alpha)} dv, \quad (3.16)$$

where $\alpha = \alpha_{\|\mathbf{w}\|^2}$ and $\beta = \beta_{\|\mathbf{w}\|^2}$ are calculated by (3.12).

In [58], we have a useful approximation for the bit error probability on an M-QAM schema. Considering coherent detection, we can state that

$$P_e^{QAM}(\gamma) \approx \frac{4}{\log_2 \mathcal{M}} Q \left(\sqrt{\frac{3\gamma \log_2 \mathcal{M}}{\mathcal{M} - 1}} \right) \quad (3.17)$$

By using the approximation in (3.17), we propose an upper bound for the bit error probability for the transmission of M -QAM symbols under Gamma fading by applying the Chernoff bound $Q(x) < -\frac{1}{2}e^{-\frac{1}{2}x^2}$ and solving the integral formula in (3.16). The proposed bound for error probability can be calculated as

$$\bar{P}_e^{QAM}(\gamma) < \frac{1.38629 \left(\frac{2.16404\gamma \log(\mathcal{M})}{(\mathcal{M}-1)\beta_{\|\mathbf{w}\|^2}} + 1 \right)^{-\alpha_{\|\mathbf{w}\|^2}}}{\log(\mathcal{M})} \quad (3.18)$$

The gamma approximation for the resulting fading coefficient is adequate and works even for small values of N and M when we consider the scenario without phase errors, as in Figure 3.1, and in the case where we have the Von Mises distributed phase errors as shown in Figure 3.2.

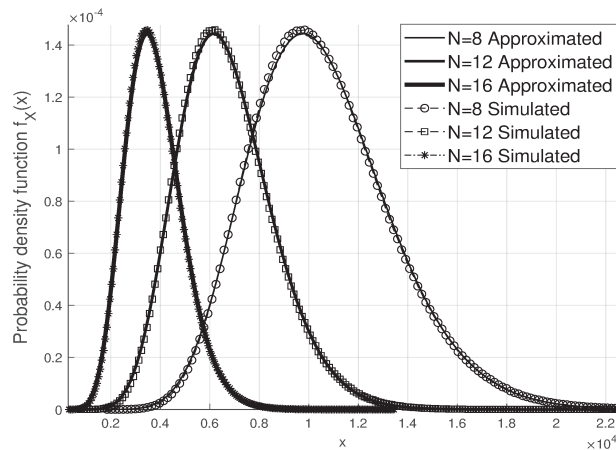


Figure 3.1: Approximated Gamma Distribution of $\|\mathbf{w}\|^2$ without phase errors.

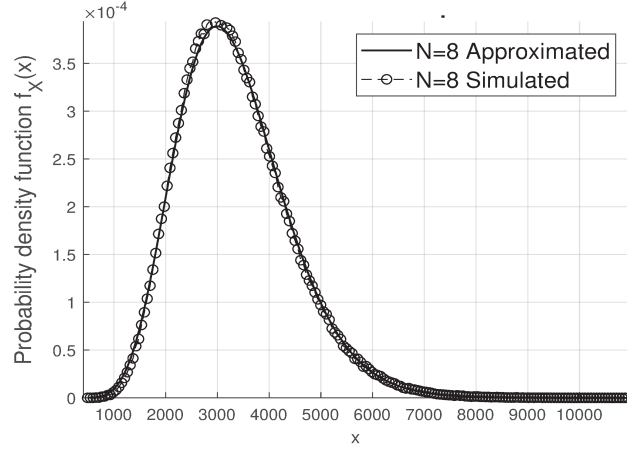


Figure 3.2: Approximated Gamma Distribution of $\|\mathbf{w}\|^2$ with Von Mises $\kappa = 2$ errors.

As we can see in Figure 3.3 the Kullback-Leibler divergence decays with the number of reflectors at the LIS and the distribution is well represented by the proposed gamma approximation.

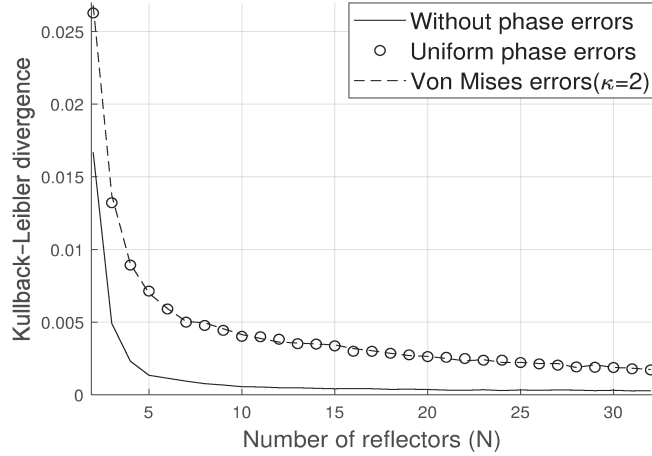


Figure 3.3: Kullback–Leibler divergence for the fading squared magnitude.

3.5 Simulated Results

We have simulated the bit error probability and generated the fading coefficients of all channels using the Monte Carlo method with 10^6 iterations. We have assumed that the phase errors follow the uniform or the Von Mises distribution. To calculate the error probability, we have solved numerically the integral in (3.16) and compared it with the Monte Carlo simulation.

Figure 3.1 shows the simulated bit error rate when there are no phase errors. As it can be observed, the simulation is very close to the analytical bit error probability. Moreover, as the

number of LIS reflectors increases, the bit error probability decreases faster concerning the SNR. This result is valid even for small values of N , for example, for $N = 8$.

On the other hand, when the phase error is uniformly distributed, as shown in Figure 3.2, the bit error probability increases significantly compared to the scenario where there are no phase errors. Again, we can observe that the analytical curve matches perfectly the simulated results, even for a small number of antennas or a small number of elements at the LIS.

It is worth mentioning that a uniform phase error, as pointed out by [2], may mean that the LIS's channel estimation or phase correction was not so effective since large and small phase errors are equiprobable.

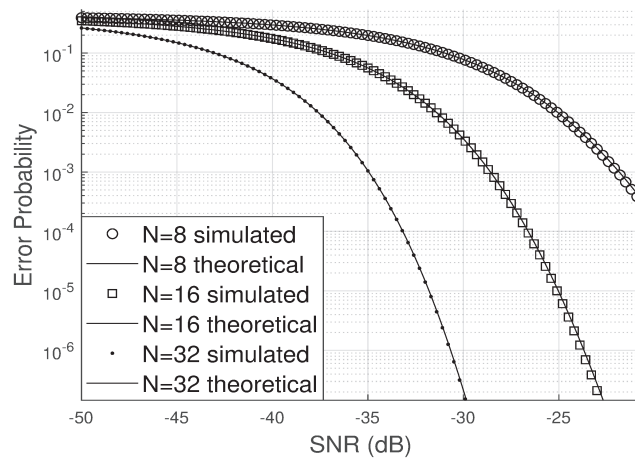


Figure 3.1: Error probability without phase errors.

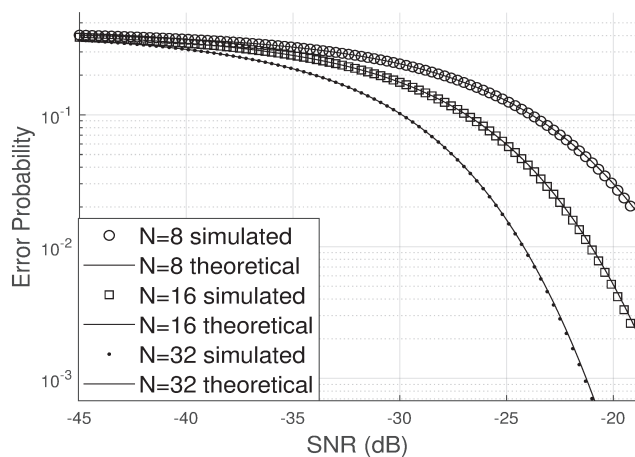


Figure 3.2: Error probability for uniformly distributed phase errors.

Comparing Figures 3.2 and 3.3, we can see that the error probability is smaller when $\kappa > 0$. The occurrence of small errors is more probable than large errors ($\pm\pi$).

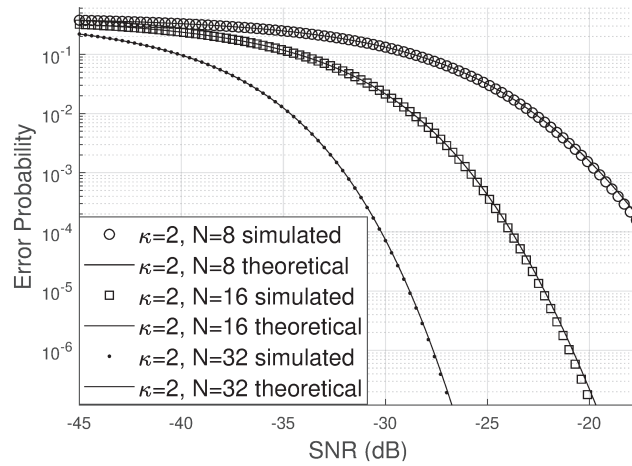


Figure 3.3: Error probability for Von Mises distributed phase errors.

Figure 3.4 shows how the bit error probability behaves as the concentration parameter varies for SNR of -25 dB. It is clear that the rate decreases as κ increases. Therefore, the κ parameter of the LIS can be considered a qualitative parameter of the phase correction performed by the reflectors for a specific channel estimation method.

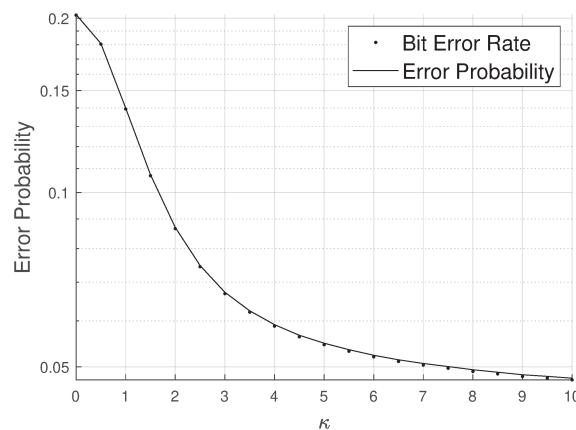


Figure 3.4: Error probability varying the Von Mises concentration parameter.

In Figure 3.5, we vary the size of the antenna array at BS and note that the bit error rate decreases significantly when M increases. Furthermore, our approximation is valid for both large and small values of M .

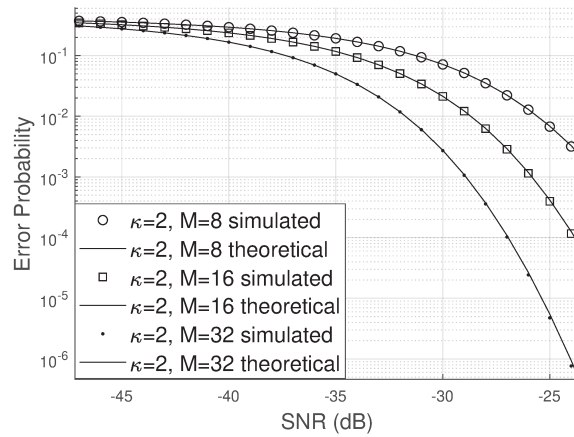


Figure 3.5: Error probability varying the size of the antenna array.

Although the numerical calculation of the analytical expression of the bit error probability is computationally fast, it may still be interesting to use a direct expression that does not involve solving numerical integrals. The proposed upper bound is very close to the simulated results, as we can see in Figure 3.6.

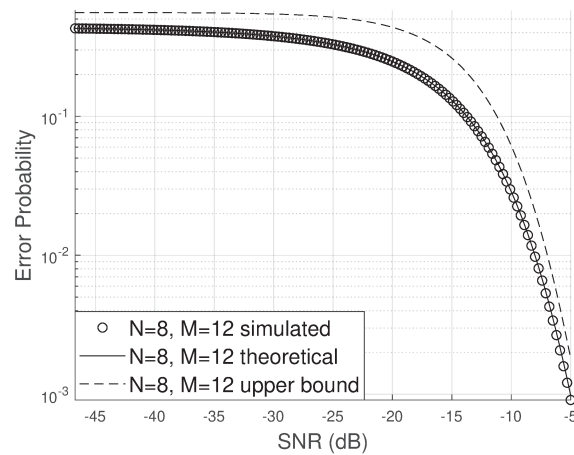


Figure 3.6: Proposed upper bound for the error probability.

Figure 3.7 shows the influence of the direct link in the bit error probability. In this figure, we have assumed that the direct link is 10dB and 30dB larger than the two indirect links. As it can be seen, when the direct link is strong, the error probability decays quickly with the increase of the SNR, on the other hand, when the direct link is weak, the bit error probability requires a larger SNR to decrease.

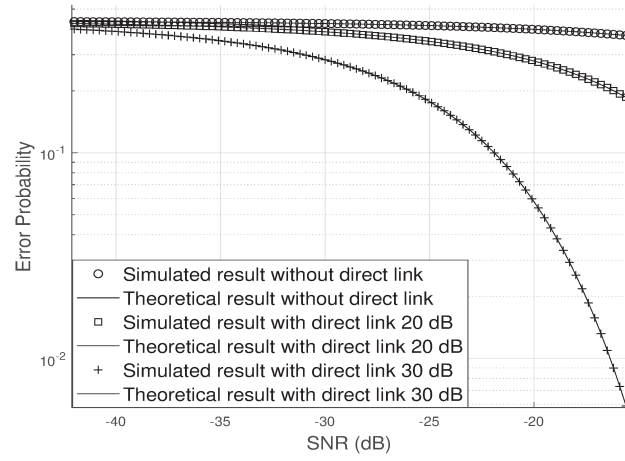


Figure 3.7: Effect of the direct link in the bit error probability.

4 Conclusion

In this work, we have proposed an approximated and upper bound expressions for calculating the bit error probability of LIS-assisted systems. We have considered BPSK and M -QAM modulations under the effect of Nakagami- m and Rayleigh fading channels. We have analyzed different scenarios regarding the Nakagami m parameter, the concentration parameter κ , the number of antennas at the base station M and the number of reflecting elements n . In short, the BER decreases when at least one of these parameters increases. All the results were validated by numerical simulations and have shown an excellent agreement. We have obtained the exact distribution of the channel coefficient for $n < 4$. However, as the exact formula gets too intricate for large values of n , we have employed a Gaussian approximation for the in-phase and quadrature components. The approximation for the PDF of $|H|$ converges very fast, and even for low values of n , the mean square error is small.

The fading coefficients of the overall channel involved in the massive MIMO scenario, considering the antenna array and the LIS can be modelled as a Gamma random variable even for a small number of antennas. We have proved the accuracy of our approximation through the Kullback-Leibler divergence even when the phase error follows either the uniform or the Von Mises distribution with arbitrary concentration parameter. In the absence of phase error, the divergence between the simulated distribution and the proposed analytical approach decreases even faster with the increase of the number of reflectors at the LIS.

Future works may include the analysis of the LIS operating in Nakagami- m fading channels in a multiuser case or antenna array scenario, and also is possible to explore the performance of the LIS aided system by means of the spectral efficiency. The existence of eavesdropper links can be considered to evaluate the secrecy rate and secrecy outage probability, these measures can improve the contribution for the LIS design.

5 Appendix

5.1 Error probability for BPSK systems with Large Intelligent Surfaces communicating through double-Nakagami Fading channels

5.1.1 Mean and Variance of C

The mean value of C is given by

$$\mu_C = E[C] = E \left[\sum_{k=1}^n \frac{1}{n} |H_{12k}| \cos \theta_k \right]. \quad (5.1)$$

Assuming that all coefficients are independent and have the same statistics, the following can be written

$$\begin{aligned} \mu_C &= n \times \frac{1}{n} \times E[|H_{12k}| \cos \theta_k] \\ &= \mu_1 \mu_2 \left(\frac{I_1(\kappa)}{I_0(\kappa)} \right), \end{aligned} \quad (5.2)$$

in which $\mu_1 = E[H_{1k}]$ and $\mu_2 = E[H_{2k}]$. The variance of C is given by

$$\sigma_C^2 = \text{var} \left(\sum_{k=1}^n \frac{1}{n} |H_{12k}| \cos \theta_k \right). \quad (5.3)$$

Note that the variance computation in (5.3) involves the product of two independent variables. Let the variables u and v be independent. Therefore, the variance of the product is given by $\text{var}(uv) = \text{var}(u)\text{var}(v) + \text{var}(u)E[v]^2 + \text{var}(v)E[u]^2$ [52]. Additionally, since all the variables are independent, the following can be written

$$\begin{aligned} \sigma_C^2 &= \frac{1}{n} \text{var}(|H_{12k}| \cos \theta_k) \\ &= \frac{1}{n} (\sigma_{12}^2 \sigma_{C_k}^2 + \sigma_{12}^2 \mu_{C_k}^2 + \sigma_{C_k}^2 \mu_{12}^2), \end{aligned} \quad (5.4)$$

whose parameters can be calculated as follows

$$\sigma_{12}^2 = \sigma_1^2 \sigma_2^2 + \mu_1^2 \sigma_2^2 + \mu_2^2 \sigma_1^2, \quad (5.5)$$

in which $\sigma_1^2 = \text{var}(H_{1k})$ and $\sigma_2^2 = \text{var}(H_{2k})$,

$$\sigma_{C_k}^2 = E[\cos^2 \theta_k] - E^2[\cos \theta_k], \quad (5.6)$$

$$\mu_{C_k} = E[\cos \theta_k] = \alpha_1 = \frac{I_1(\kappa)}{I_0(\kappa)}, \quad (5.7)$$

$$E[\cos^2 \theta_k] = \frac{1}{2} + \frac{1}{2}E[\cos 2\theta_k] = \frac{1}{2} + \frac{1}{2}\alpha_2. \quad (5.8)$$

and

$$\sigma_{C_k}^2 = \frac{1}{2} + \frac{1}{2} \frac{I_2(\kappa)}{I_0(\kappa)} + \left(\frac{I_1(\kappa)}{I_0(\kappa)} \right)^2. \quad (5.9)$$

Therefore, the variance of C is defined as

$$\begin{aligned} \sigma_C^2 &= \frac{1}{2n} \sigma_{12}^2 \left(1 + \frac{I_2(\kappa)}{I_0(\kappa)} + 4 \left[\frac{I_1(\kappa)}{I_0(\kappa)} \right]^2 \right) + \dots \\ &\quad \dots + \mu_1 \mu_2 \frac{1}{2n} \left(1 + \frac{I_2(\kappa)}{I_0(\kappa)} \right). \end{aligned} \quad (5.10)$$

5.1.2 Mean and Variance of S

The mean value of S can be written as

$$\begin{aligned} \mu_S &= E[S] = E \left[\sum_{k=1}^n \frac{1}{n} |H_{12k}| \sin \theta_k \right] \\ &= \frac{1}{n} \times n \times \mu_1 \mu_2 E[\sin \theta_k], \end{aligned} \quad (5.11)$$

Using the same assumptions as in the previous case, the mean value of S can be calculated as

$$\mu_{S_k} = E[\sin \theta_k] = \beta_1 = 0. \quad (5.12)$$

Therefore,

$$\mu_S = 0 \quad (5.13)$$

On the other hand, the variance of S can be computed as

$$\begin{aligned} \sigma_S^2 &= \text{var} \left(\sum_{k=1}^n \frac{1}{n} |H_{12k}| \sin \theta_k \right) \\ &= \frac{1}{n} (\sigma_{12}^2 \sigma_{S_k}^2 + \sigma_{12}^2 \mu_{S_k}^2 + \sigma_{S_k}^2 \mu_{12}^2), \end{aligned} \quad (5.14)$$

whose parameters can be calculated as follows

$$\sigma_{S_k}^2 = E[\sin^2 \theta_k] - E^2[\sin \theta_k]$$

$$= \frac{1}{2} - \frac{1}{2} \frac{I_2(\kappa)}{I_0(\kappa)} \quad (5.15)$$

$$E[\sin^2 \theta_k] = \frac{1}{2} - \frac{1}{2} E[\cos 2\theta_k] = \frac{1}{2} - \frac{1}{2} \alpha_2.$$

Therefore, the variance of S is defined as

$$\sigma_S^2 = \frac{1}{2n} \sigma_{12}^2 \left(1 - \frac{I_2(\kappa)}{I_0(\kappa)}\right) + \frac{1}{2n} (\mu_1 \mu_2)^2 \left(1 - \frac{I_2(\kappa)}{I_0(\kappa)}\right). \quad (5.16)$$

5.1.3 Mean of the product of C and S

This appendix shows that C and S are uncorrelated. Considering a possible correlation between C and S , the bivariate Gaussian joint distribution can be written as

$$f_{C,S}(x, y) = \frac{1}{2\pi\sigma_C\sigma_S\sqrt{1-\rho^2}} e^{-\frac{1}{2\sqrt{1-\rho^2}} \left(\frac{(x-\mu_C)^2}{\sigma_C^2} + \frac{(y-\mu_S)^2}{\sigma_S^2} - \frac{2\rho(x-\mu_C)(y-\mu_S)}{\sigma_C\sigma_S} \right)} \quad (5.17)$$

where ρ is defined as [52]

$$\rho = \frac{E[CS] - E[C]E[S]}{\sigma_C\sigma_S} \quad (5.18)$$

As it has been calculated from (5.13), the term $E[S] = 0$, that is, the second term of the numerator of (5.18) is zero. Therefore in order to prove that $\rho = 0$, we need to compute the mean of the product between C and S and show that is also zero.

Departing from (2.11) and (2.12), the mean of the product between C and S can be written as

$$E[CS] = E \left[\sum_{i=1}^n \sum_{j=1}^n R_i R_j \cos(\theta_i) \sin(\theta_j) \right] \quad (5.19)$$

Since R_k is independent of θ_k for all k , then

$$E[CS] = 2 \sum_{i=1}^n \sum_{j>i}^n E[R_i R_j] E[\cos(\theta_i) \sin(\theta_j)] + \sum_{k=1}^n E[R_k^2] E[\sin(\theta_k) \cos(\theta_k)] \quad (5.20)$$

In the sequel, the following equalities will be proven $E[\cos(\theta_i) \sin(\theta_j)] = 0$ and $E[\sin(\theta_i) \cos(\theta_i)] = 0$, and therefore (5.20) will be null.

Using the very definition of the mean, the term $E[\cos(\theta_i) \sin(\theta_j)]$ can be computed as

$$E[\cos(\theta_i) \sin(\theta_j)] = \int_0^{2\pi} \int_0^{2\pi} \cos(\theta_i) \sin(\theta_j) \frac{e^{\kappa \cos(\theta_i)}}{2\pi I_0(\kappa)} \frac{e^{\kappa \cos(\theta_j)}}{2\pi I_0(\kappa)} d\theta_i d\theta_j = 0, \quad (5.21)$$

in the same way, the mean with respect to θ_i in the second term of (5.20), can be calculated as

$$E[\cos(\theta_i) \sin(\theta_i)] = \int_0^{2\pi} \frac{\cos(\theta_i) \sin(\theta_i)}{2\pi I_0(\kappa)} e^{\kappa \cos(\theta_i)} d\theta_i = 0, \quad (5.22)$$

therefore $E[CS] = 0$ and consequently ρ , given in (5.18)), will be $\rho = 0$. From this, (5.17) can be written as in (2.15).

5.2 Large Intelligent Surfaces Communicating Through Massive MIMO Rayleigh Fading Channels

5.2.1 Mean of w_k Given in (3.5)

Departing from (3.5), the mean of the each total fading coefficient can be calculated as

$$E[w_k] = E \left[\sum_{i=1}^N |g_{ki}| |h_i^{LIS}| + h_k^{BS} \right] \quad (5.23)$$

since $|g_{ki}|$ and $|h_i^{LIS}|$ are independent and equally probable on the summation variable.

So,

$$E[w_k] = N \times E[|g_{ki}|] E[|h_i^{LIS}|] + E[h_k^{BS}] \quad (5.24)$$

Since $E[h_k^{BS}] = 0$,

$$E[w_k] = N \times E[|g_{ki}|] E[|h_i^{LIS}|] \quad (5.25)$$

The terms $|g_{ki}|$ and $|h_i^{LIS}|$ are Rayleigh distributed, since the variables g_{ki} and h_i^{LIS} are zero mean with variances σ_1^2 and σ_2^2 , respectively. Therefore

$$E[|g_{ki}|] = \sigma_1 \sqrt{\frac{\pi}{2}}, \quad E[|h_i^{LIS}|] = \sigma_2 \sqrt{\frac{\pi}{2}}. \quad (5.26)$$

Let $w_k = c_k + js_k$, where c_k and s_k are the in-phase and quadrature components of the fading coefficient with respect to the antenna k . Also, let $\mu_{c_k} = E[c_k]$ and $\mu_{s_k} = E[s_k] = 0$.

Then,

$$E[w_k] = \mu_{c_k} = N \frac{\pi}{2} \sigma_1 \sigma_2. \quad (5.27)$$

5.2.2 Variance of w_k Given in (3.5)

The variance of w_k is given by

$$\text{var}(w_k) = E[(c_k + js_k)(c_k - js_k)] - (E[(c_k + js_k)])^2 = \text{var}(c_k) + \text{var}(s_k), \quad (5.28)$$

where

$$\text{var}(c_k) = \text{var} \left(\sum_{i=1}^N |g_{ki}| |h_i^{LIS}| + C_{BS,k} \right), \quad (5.29)$$

and can be expanded as

$$\text{var}(c_k) = \text{var} \left(\sum_{i=1}^N |g_{ki}| |h_i^{LIS}| \right) + \text{var}(C_{BS,k}) + 2 \left(E \left[C_{BS,k} \sum_{i=1}^N |g_{ki}| |h_i^{LIS}| \right] \right)^2, \quad (5.30)$$

The first term of (5.30) can be written as

$$\text{var} \left(\sum_{i=1}^N |g_{ki}| |h_i^{LIS}| \right) = N \text{var}(|g_{ki}| |h_i^{LIS}|) \quad (5.31)$$

Note in (5.31) that it is necessary to compute the variance of the product of two random variables. Let X and Y , two independent random variables, then $\text{var}(XY) = \text{var}(X)\text{var}(Y) + \text{var}(X)E[Y]^2 + \text{var}(Y)E[X]^2$ and then.

$$\begin{aligned} \text{var}(|g_{ki}| |h_i^{LIS}|) &= \\ \text{var}(|g_{ki}|) \times \text{var}(|h_i^{LIS}|) &+ \text{var}(|g_{ki}|) (E[|h_i^{LIS}|])^2 + \text{var}(|h_i^{LIS}|) (E[|g_{ki}|])^2 \end{aligned} \quad (5.32)$$

Since $|g_{ki}|$ and $|h_i^{LIS}|$ are Rayleigh distributed,

$$\text{var}(|g_{ki}|) = \frac{4 - \pi}{2} \sigma_1^2, \quad \text{var}(|h_i^{LIS}|) = \frac{4 - \pi}{2} \sigma_2^2 \quad (5.33)$$

and so, after some simplifications, we have that

$$\text{var}(|g_{ki}| |h_i^{LIS}|) = \frac{16 - \pi^2}{4} (\sigma_1 \sigma_2)^2 \quad (5.34)$$

Since $E[C_{BS,k}] = 0$ and the terms $C_{BS,k}$ and $\sum_{i=1}^N |g_{ki}| |h_i^{LIS}|$ are independent, then

$$\text{var}(c_k) = N \frac{16 - \pi^2}{4} (\sigma_1 \sigma_2)^2 + \sigma_3^2 \quad (5.35)$$

therefore the variance of w_k is given as

$$\text{var}(w_k) = N \frac{16 - \pi^2}{4} (\sigma_1 \sigma_2)^2 + 2\sigma_3^2. \quad (5.36)$$

5.2.3 Expected Value of $\|\mathbf{w}\|^2$

The expected value of $\|\mathbf{w}\|^2$ can be calculated by

$$E[\|\mathbf{w}\|^2] = E\left[\sum_{k=1}^M |w_k|^2\right] = ME[|w_k|^2] \quad (5.37)$$

With $E[w_k]$ and $\text{var}(w_k)$, we can calculate $E[|w_k|^2]$ as $E[|w_k|^2] = \text{var}(w_k) + (E[w_k])^2$.

Therefore, we have

$$E[|w_k|^2] = N \frac{16 - \pi^2}{4} (\sigma_1 \sigma_2)^2 + 2\sigma_3^2 + \left(N \frac{\pi}{2} \sigma_1 \sigma_2\right)^2, \quad (5.38)$$

so the mean of the overall channel fading coefficient is

$$\mu_{\|\mathbf{w}\|^2} = E[\|\mathbf{w}\|^2] = M \left(N \frac{16 - \pi^2}{4} (\sigma_1 \sigma_2)^2 + 2\sigma_3^2 + \left(N \frac{\pi}{2} \sigma_1 \sigma_2\right)^2 \right) \quad (5.39)$$

5.2.4 Correlation between the Fading Coefficients

Since the real and imaginary parts of the fading coefficients, without phase errors, are uncorrelated, we analyze only the correlation between the real parts as follows.

$$\rho_{c_i, c_k} = \frac{E[c_i c_k] - E[c_i]E[c_k]}{\sqrt{\text{var}(c_i)\text{var}(c_k)}}. \quad (5.40)$$

Since $\text{var}(c_i) = \text{var}(c_k)$ and $E[c_i] = E[c_k]$,

$$\rho_{c_i, c_k} = \frac{E[c_i c_k] - \mu_{c_k}^2}{\text{var}(c_k)} \quad (5.41)$$

where

$$E[c_i c_k] = E\left[\left(\sum_{l=1}^N |g_{il}| |h_l^{LIS}| + C_{BS,i}\right) \times \left(\sum_{m=1}^N |g_{km}| |h_m^{LIS}| + C_{BS,k}\right)\right], \quad (5.42)$$

and simplifies to

$$E[c_i c_k] = E\left[\sum_{l=1}^N \sum_{m=1}^N |g_{il}| |g_{km}| |h_l^{LIS}| |h_m^{LIS}|\right] + E[C_{BS,i} C_{BS,k}] + E[C_{BS,i}] \left(\sum_{m=1}^N |g_{km}| |h_m^{LIS}| + C_{BS,k}\right) + E[C_{BS,k}] \left(\sum_{l=1}^N |g_{il}| |h_l^{LIS}| + C_{BS,i}\right). \quad (5.43)$$

Since $E[C_{BS,i}] = E[C_{BS,k}] = 0$, $E[|g_{il}|] = E[|g_{km}|]$, $E[|h_l^{LIS}|] = E[|h_m^{LIS}|]$ so

$$E[c_i c_k] = \sum_{l=1}^N \sum_{m=1}^N E[|g_{il}| |g_{km}| |h_l^{LIS}| |h_m^{LIS}|] + E[C_{BS,i} C_{BS,k}] \quad (5.44)$$

Since $|g_{il}|$ and $|g_{km}|$ are independent, therefore

$$E[|g_{il}| |g_{km}| |h_l^{LIS}| |h_m^{LIS}|] = E[|g_{il}|] E[|g_{km}|] E[|h_l^{LIS}|] E[|h_m^{LIS}|] \quad \forall l \neq m \quad (5.45)$$

and

$$l = m \Rightarrow E[|g_{il}| |g_{km}| |h_l^{LIS}| |h_m^{LIS}|] = E[|g_{il}|] E[|g_{km}|] E[|h_m^{LIS}|^2] \quad (5.46)$$

since

$$E[|h_m^{LIS}|^2] = \text{var}(|h_m^{LIS}|) + (E[|h_m^{LIS}|])^2, \quad (5.47)$$

so, we have that

$$E[|h_m^{LIS}|^2] = \frac{4-\pi}{2} \sigma_2^2 + \frac{\pi}{2} \sigma_2^2 = 2\sigma_2^2 \quad (5.48)$$

Therefore

$$\sum_{l=1}^N \sum_{m=1}^N E[|g_{il}| |g_{km}| |h_l^{LIS}| |h_m^{LIS}|] = N\pi\sigma_1^2\sigma_2^2 \left(1 + \frac{(N-1)\pi}{4}\right) \quad (5.49)$$

Since

$$E[C_{BS,i} C_{BS,k}] = \begin{cases} 0 & k \neq i \\ E[C_{BS,k}^2] = \sigma_3^2 & k = i \end{cases}$$

Therefore

$$E[c_i c_k] = \begin{cases} N\pi\sigma_1^2\sigma_2^2 \left(1 + \frac{(N-1)\pi}{4}\right) & k \neq i \\ N\pi\sigma_1^2\sigma_2^2 \left(1 + \frac{(N-1)\pi}{4}\right) + \sigma_3^2 & k = i \end{cases}$$

Since $E[c_k] = E[w_k] = N\frac{\pi}{2}\sigma_1\sigma_2$, we only need to consider the case $i \neq k$, because for $i = k$ we have that $\rho_{c_i, c_k} = \rho_{c_k, c_k} = 1$ therefore

$$\rho_{c_i, c_k} = \frac{N\pi\sigma_1^2\sigma_2^2 \left(1 + \frac{(N-1)\pi}{4}\right) - \left(N\frac{\pi}{2}\sigma_1\sigma_2\right)^2}{N\frac{16-\pi^2}{4} (\sigma_1\sigma_2)^2 + \sigma_3^2} \quad \forall i \neq k \quad (5.50)$$

by performing algebraic simplifications we have that

$$\rho_{c_i, c_k} = \frac{N\pi (\sigma_1\sigma_2)^2}{N(\pi+4) (\sigma_1\sigma_2)^2 + \frac{4}{4-\pi}\sigma_3^2} \quad \forall i \neq k \quad (5.51)$$

5.2.5 Variance of $\|\mathbf{w}\|^2$

Let $Z_k = |w_k|^2$, so the variance of the sum of the correlated random variables Z_k will be given by

$$\text{var}(\|\mathbf{w}\|^2) = \text{var}\left(\sum_{i=1}^M Z_i\right) = \sum_{i=1}^M \text{var}(Z_i) + 2 \sum_{1 \leq i < k \leq M} \text{cov}(Z_i, Z_k). \quad (5.52)$$

Since the variables have the same distribution and parameters therefore

$$\text{var}\left(\sum_{i=1}^M Z_i\right) = M \times \text{var}(Z_i) + M(M-1) \times \text{cov}(Z_i, Z_k), \quad (5.53)$$

so, the pairwise covariance can be obtained by

$$\text{cov}(Z_i, Z_k) = E[Z_i Z_k] - E[Z_i]E[Z_k] \quad (5.54)$$

where

$$E[Z_i Z_k] = E[|w_i|^2 |w_k|^2] = E[(c_i^2 + s_i^2)(c_k^2 + s_k^2)] \quad (5.55)$$

and simplifies to

$$E[Z_i Z_k] = E[c_i^2 c_k^2] + E[c_i^2 s_k^2] + E[s_i^2 c_k^2] + E[s_i^2 s_k^2] \quad (5.56)$$

Since

$$E[c_i^2 s_k^2] = E[s_i^2 c_k^2], \quad (5.57)$$

so,

$$E[Z_i Z_k] = E[c_i^2 c_k^2] + 2E[c_i^2 s_k^2] + E[s_i^2 s_k^2] \quad (5.58)$$

Considering that c_k and c_i are correlated Gaussian random variables with the same mean and variance, therefore we have that

$$E[c_i^2 c_k^2] = \int_{-\infty}^{\infty} \int_{-\infty}^{\infty} x^2 y^2 f_{c_i, c_k}(x, y) dx dy \quad (5.59)$$

where $f_{c_i, c_k}(x, y)$ is the joint probability density function of the correlated Gaussian random variables c_i and c_k .

$$E[c_i^2 c_k^2] = \mu_{c_k}^4 + 2\mu_{c_k}^2 (1 + 2\rho_{c_i, c_k}) \sigma_{c_k}^2 + (1 + 2\rho_{c_i, c_k}^2) \sigma_{c_k}^4 \quad (5.60)$$

$$E[c_i^2 c_k^2] = \begin{cases} k_1^4 \sigma_{12}^4 + 2k_1^2 \sigma_{12}^2 \left(\frac{k_1}{2\pi} a_1 a_2 \sigma_{12}^2 + \sigma_3^2 \right) + 2k_1^3 a_1 \sigma_{12}^4 + \frac{1}{2} k_1^2 \sigma_{12}^4 a_1^2 + \dots \\ \left(\frac{k_1}{2\pi} a_1 a_2 \sigma_{12}^2 + \sigma_3^2 \right)^2 & i \neq k \\ k_1^4 \sigma_{12}^4 + 6k_1^2 \sigma_{12}^2 \left(\frac{k_1}{2\pi} a_1 a_2 \sigma_{12}^2 + \sigma_3^2 \right) + 3 \left(\frac{k_1}{2\pi} a_1 a_2 \sigma_{12}^2 + \sigma_3^2 \right)^2 & i = k \end{cases}$$

Therefore $E[c_i^2 c_k^2]$ can be calculated by (5.90), where $k_1 = N \frac{\pi}{2}$, $a_1 = 4 - \pi$, $a_2 = 4 + \pi$ and $\sigma_{12} = \sigma_1 \sigma_2$.

Since c_i and s_k are independent and $E[|s_k^2|] = \text{var}(s_k)$ so we have that

$$E[c_i^2 s_k^2] = E[c_i^2] E[s_k^2] \quad (5.61)$$

Since

$$E[c_i^2] = \text{var}(c_i) + (E[c_i])^2 = \frac{k_1}{2\pi} a_1 a_2 \sigma_{12}^2 + \sigma_3^2 + k_1^2 \sigma_{12}^2,$$

so, we have that

$$E[c_i^2] = \sigma_{12}^2 \left(\frac{k_1}{2\pi} a_1 a_2 + k_1^2 \right) + \sigma_3^2,$$

Since $E[s_k^2] = \text{var}(s_k) = \sigma_3^2$, therefore

$$E[c_i^2 s_k^2] = \sigma_{123}^2 \left(\frac{k_1}{2\pi} a_1 a_2 + k_1^2 \right) + \sigma_3^4 \quad (5.62)$$

where $\sigma_{123}^2 = \sigma_1^2 \sigma_2^2 \sigma_3^2$.

The fourth order moment $E[s_k^4]$ of a Gaussian random variable is well known in the literature and can be calculated by

$$E[s_k^4] = (E[s_k])^4 + 2(E[s_k])^2 \text{var}(s_k) + 3(\text{var}(s_k))^2 \quad (5.63)$$

Since $E[s_k] = 0$, therefore

$$E[s_k^4] = 3\sigma_3^4 \quad (5.64)$$

$$E[Z_i Z_k] =$$

$$\left\{ \begin{array}{ll} k_1^4 \sigma_{12}^4 + 2k_1^2 \sigma_{12}^2 \left(\frac{k_1}{2\pi} a_1 a_2 \sigma_{12}^2 + \sigma_3^2 \right) + 2k_1^3 a_1 \sigma_{12}^4 + \frac{1}{2} k_1^2 \sigma_{12}^4 a_1^2 + \dots & \\ \left(\frac{k_1}{2\pi} a_1 a_2 \sigma_{12}^2 + \sigma_3^2 \right)^2 + 2\sigma_{123}^2 \left(\frac{k_1}{2\pi} a_1 a_2 + k_1^2 \right) + 3\sigma_3^4 & i \neq k \\ \\ k_1^4 \sigma_{12}^4 + 6k_1^2 \sigma_{12}^2 \left(\frac{k_1}{2\pi} a_1 a_2 \sigma_{12}^2 + \sigma_3^2 \right) + 3 \left(\frac{k_1}{2\pi} a_1 a_2 \sigma_{12}^2 + \sigma_3^2 \right)^2 + \dots & \\ 2\sigma_{123}^2 \left(\frac{k_1}{2\pi} a_1 a_2 + k_1^2 \right) + 5\sigma_3^4 & i = k \end{array} \right. \quad (5.65)$$

With the expected value $E[Z_i Z_k]$, the expected value of $Z_k = |w_k|^2$ and the consideration that $E[Z_i] = E[Z_k] \forall i \forall k$, the covariance between Z_i and Z_k can be obtained by

$$\text{cov}(Z_i, Z_k) = E[Z_i Z_k] - (E[Z_k])^2 \quad (5.66)$$

Note that $\text{var}(Z_k) = \text{cov}(Z_k, Z_k)$, so the variance of $\|\mathbf{w}\|^2$ can be obtained by

$$\sigma_{\|\mathbf{w}\|^2}^2 = \text{var}(\|\mathbf{w}\|^2) = M \text{cov}(Z_k, Z_k) + M(M-1) \text{cov}(Z_i, Z_k) \quad (5.67)$$

By substituting the terms $E[Z_i Z_k]$ and $E[Z_k]$, given in (5.65) and (5.27), in the equation (5.67), we have that the analytical expression of the variance in (5.68).

$$\begin{aligned} \sigma_{\|\mathbf{w}\|^2}^2 = & M \left(k_2^4 + 2k_2^2(k_3 + \sigma_3^2) + 2k_1 k_4^2 a_1 \frac{1}{2} k_4^2 a_1^2 + (k_3 + \sigma_3^2)^2 + \right. \\ & \left. 2\sigma_3^2(k_3 + k_2^2) + 3\sigma_3^4 - (k_3 + 2\sigma_3^2 + k_2^2)^2 \right) + \dots \\ & M(M+1) \left(k_2^4 + 6k_2^2(k_3 + \sigma_3^2) + 3(k_3 + \sigma_3^2)^2 + 2(k_3 + k_2^2) + 5\sigma_3^4 - (k_3 + 2\sigma_3^2 + k_2^2)^2 \right) \end{aligned} \quad (5.68)$$

where

$$k_2 = k_1 \sigma_{12}, \quad k_3 = \frac{k_1}{2\pi} a_1 a_2 \sigma_{12}^2, \quad k_4 = k_1 \sigma_{12}^2$$

5.3 Mean and Variance of the Overall Channel Fading Coefficient with Von Mises Distributed Phase Errors

5.3.1 Mean of \tilde{w}_k

Let $\tilde{w}_k = \tilde{c}_k + j\tilde{s}_k$ be the fading coefficient with respect to the antenna k when phase errors occurs at the LIS. To obtain the mean of \tilde{w}_k we need to calculate the mean of \tilde{c}_k and \tilde{s}_k .

The mean value of the in-phase fading component \tilde{c}_k is

$$E[\tilde{c}_k] = N \frac{\pi}{2} \sigma_{12} \alpha_1 \quad (5.69)$$

and the quadrature component mean $E[\tilde{s}_k]$ is

$$E[\tilde{s}_k] = E \left[\sum_{i=1}^N |g_{ki}| |h_i^{LIS}| \sin \delta_{ki} + \tilde{S}_k^{BS} \right] \quad (5.70)$$

using the linearity of the expected value we can rewrite the equation as

$$E[\tilde{s}_k] = \sum_{i=1}^N E [|g_{ki}| |h_i^{LIS}| \sin \delta_{ki}] + E [\tilde{S}_k^{BS}] \quad (5.71)$$

since $\beta_1 = 0$, so

$$E[\tilde{s}_k] = N \frac{\pi}{2} \sigma_{12} \beta_1 = 0 \quad (5.72)$$

Therefore we can calculate the mean of the overall fading coefficient, for the antenna k by using

$$E[\tilde{w}_k] = E[\tilde{c}_k] + E[\tilde{s}_k] = N \frac{\pi}{2} \sigma_{12} \alpha_1. \quad (5.73)$$

5.3.2 Variance of the In-Phase and Quadrature Components

To obtain the variance of \tilde{w}_k we need to calculate the variance of \tilde{c}_k and \tilde{s}_k . The variance of the quadrature component is

$$\text{var}(\tilde{s}_k) = N \text{var}(|g_{ki}| |h_i^{LIS}| \sin \delta_{ki}) + \sigma_3^2, \quad (5.74)$$

where

$$\begin{aligned} \text{var}(|g_{ki}| |h_i^{LIS}| \sin \delta_{ki}) &= \text{var}(|g_{ki}| |h_i^{LIS}|) \text{var}(\sin \delta_{ki}) + \dots \\ &\text{var}(\sin \delta_{ki}) (E[|g_{ki}| |h_i^{LIS}|])^2 + \text{var}(|g_{ki}| |h_i^{LIS}|) (E[\sin \delta_{ki}])^2 \end{aligned} \quad (5.75)$$

and simplifies to

$$\begin{aligned} \text{var}(|g_{ki}| |h_i^{LIS}| \cos \delta_{ki}) &= \text{var}(|g_{ki}| |h_i^{LIS}|) \text{var}(\cos \delta_{ki}) + \dots \\ &\text{var}(\cos \delta_{ki}) (E[|g_{ki}| |h_i^{LIS}|])^2 + \text{var}(|g_{ki}| |h_i^{LIS}|) (E[\cos \delta_{ki}])^2. \end{aligned} \quad (5.76)$$

To compute the variance of the in-phase and quadrature components we need to calculate closed expressions for the trigonometric moments of the Von Mises random variable.

The expected value of the sine of a Von Mises distributed phase error is given as

$$\begin{aligned}\text{var}(\sin \delta_{ki}) &= E[\sin^2 \delta_{ki}] - (E[\sin \delta_{ki}])^2 \\ &= \frac{1}{2} (1 - E[\cos 2\delta_{ki}]) - (E[\sin \delta_{ki}])^2 \\ &= \frac{1}{2} (1 - \alpha_2) - \beta_1^2\end{aligned}\quad (5.77)$$

Since $\beta_1 = 0$, so

$$\text{var}(\sin \delta_{ki}) = \frac{1}{2} (1 - \alpha_2) \quad (5.78)$$

The expected value of the cosine of a Von Mises variable can be calculated by

$$\text{var}(\cos \delta_{ki}) = E[\cos^2 \delta_{ki}] - (E[\cos \delta_{ki}])^2, \quad (5.79)$$

or, using a trigonometric substitution,

$$\text{var}(\cos \delta_{ki}) = \frac{1}{2} (1 + E[\cos 2\delta_{ki}]) - \alpha_1^2, \quad (5.80)$$

In terms of the the characteristic function, we have

$$\text{var}(\cos \delta_{ki}) = \frac{1}{2} (1 + \alpha_2) - (\alpha_1)^2 \quad (5.81)$$

So the variance of \tilde{s}_k is

$$\text{var}(\tilde{s}_k) = N \left[\frac{16 - \pi^2}{8} \sigma_{12}^2 (1 - \alpha_2) \frac{\pi^2}{8} \sigma_{12}^2 (1 - \alpha_2) \right] + \sigma_3^2 \quad (5.82)$$

and simplifies to

$$\text{var}(\tilde{s}_k) = N (2\sigma_{12}^2 (1 - \alpha_2)) + \sigma_3^2. \quad (5.83)$$

The variance of the in-phase fading coefficient will be

$$\begin{aligned}\text{var}(\tilde{c}_k) &= N \left[\frac{16 - \pi^2}{4} \sigma_{12}^2 \left(\frac{1}{2} (1 + \alpha_2) - \alpha_1^2 \right) + \dots \right. \\ &\quad \left. \alpha_1^2 \frac{16 - \pi^2}{4} \sigma_{12}^2 + \left(\frac{1}{2} (1 + \alpha_2) - \alpha_1^2 \right) \frac{\pi^2}{4} \sigma_{12}^2 \right] + \sigma_3^2\end{aligned}\quad (5.84)$$

and simplifies to

$$\text{var}(\tilde{c}_k) = \sigma_3^2 + N \left[2\sigma_{12}^2 (1 + \alpha_2) - \frac{\pi^2}{4} \alpha_1^2 \sigma_{12}^2 \right] \quad (5.85)$$

5.3.3 Mean of $|\tilde{w}_k|^2$

To compute the variance of the total fading coefficient we need the mean value of the squared fading coefficients.

The mean of the squared in-phase component is given as

$$E[\tilde{c}_k^2] = \sigma_3^2 + N \left[2\sigma_{12}^2(1 + \alpha_2) - \frac{\pi^2}{4}\alpha_1^2\sigma_{12}^2 \right] + \left(N\frac{\pi}{2}\sigma_{12}\alpha_1 \right)^2. \quad (5.86)$$

The expected value of the squared quadrature component can be written as

$$E[\tilde{s}_k^2] = \text{var}(\tilde{s}_k) = N (2\sigma_{12}^2 (1 - \alpha_2)) + \sigma_3^2 \quad (5.87)$$

Therefore, the mean squared magnitude of the overall fading with respect to the antenna k is given as

$$E[|\tilde{w}_k|^2] = N \left[2\sigma_{12}^2(1 + \alpha_2) - \frac{\pi^2}{4}\alpha_1^2\sigma_{12}^2 \right] + \left(N\frac{\pi}{2}\sigma_{12}\alpha_1 \right)^2 + N (2\sigma_{12}^2 (1 - \alpha_2)) + 2\sigma_3^2 \quad (5.88)$$

and simplifies to

$$E[|\tilde{w}_k|^2] = 4N(1 + \alpha_2)\sigma_{12}^2 + 2\sigma_3^2 \quad (5.89)$$

5.3.4 Correlation between the Fading Coefficients

The real and imaginary parts of the fading coefficients are uncorrelated, however we need to compute the correlation coefficient between the real parts.

The expected value of the product of two different in-phase coefficients can be written as

$$E[\tilde{c}_i\tilde{c}_k] = E \left[\left(\sum_{l=1}^N |g_{il}||h_l^{LIS}| \cos \delta_{il} + \tilde{C}_{BS,i} \right) \times \left(\sum_{m=1}^N |g_{km}||h_m^{LIS}| \cos \delta_{km} + \tilde{C}_{BS,k} \right) \right] \quad (5.90)$$

since all the variables have the same distribution and parameters, therefore if $l \neq m$, so all the summation variables are independent, and in addition $E[\tilde{C}_{BS,k}] \forall k$ and the variables $\tilde{C}_{BS,i}$ and $\tilde{C}_{BS,k}$ are independent $\forall i \neq k$, therefore

$$E[\tilde{c}_i\tilde{c}_k] = E[\tilde{C}_{BS,i}\tilde{C}_{BS,k}] + \sum_{l=1}^N \sum_{m=1}^N E[|g_{il}||g_{km}||h_l^{LIS}||h_m^{LIS}| \cos \delta_{il} \cos \delta_{km}] \quad (5.91)$$

and

$$l \neq m \Rightarrow E [|g_{il}| |g_{km}| |h_l^{LIS}| |h_m^{LIS}| \cos \delta_{il} \cos \delta_{km}] = E [|g_{km}|^2] E [|h_m^{LIS}|^2] E [\cos \delta_{km}]^2 =$$

$$\left(\sigma_1 \sqrt{\frac{\pi}{2}} \right)^2 \left(\sigma_2 \sqrt{\frac{\pi}{2}} \right)^2 \alpha_1^2 = \frac{\pi^2}{4} \sigma_{12}^2 \alpha_1^2 \quad (5.92)$$

and also

$$l = m, i \neq k \Rightarrow E [|g_{il}| |g_{km}| |h_l^{LIS}| |h_m^{LIS}| \cos \delta_{il} \cos \delta_{km}] = E [|g_{km}|^2] E [|h_m^{LIS}|^2] E [\cos \delta_{im}] E [\cos \delta_{km}] =$$

$$\frac{\pi}{2} \sigma_1^2 (2\sigma_2)^2 \alpha_1^2 = \pi \sigma_{12}^2 \alpha_1^2, \quad (5.93)$$

$$l = m, i = k \Rightarrow E [|g_{il}| |g_{km}| |h_l^{LIS}| |h_m^{LIS}| \cos \delta_{il} \cos \delta_{km}] = E [|g_{km}|^2] E [|h_m^{LIS}|^2] E [\cos^2 \delta_{km}] =$$

$$2\sigma_1^2 2\sigma_2^2 \frac{1}{2} (1 - \alpha_2) \quad (5.94)$$

therefore

$$E[\tilde{c}_i \tilde{c}_k] = \begin{cases} N(N-1) \left(\frac{\pi^2}{4} \sigma_{12}^2 \alpha_1^2 \right) + N (\pi \sigma_{12}^2 \alpha_1^2) & i \neq k \\ N (2\sigma_1^2 2\sigma_2^2 \frac{1}{2} (1 - \alpha_2)) + \sigma_3^2 + \dots & \\ N(N-1) \left(\frac{\pi^2}{4} \sigma_{12}^2 \alpha_1^2 \right) & i = k \end{cases}$$

and the correlation for $i \neq k$ is given as

$$\rho_{\tilde{c}_i \tilde{c}_k} = \frac{N(N-1) \left(\frac{\pi^2}{4} \sigma_{12}^2 \alpha_1^2 \right) + N (\pi \sigma_{12}^2 \alpha_1^2) - (N \frac{\pi}{2} \sigma_{12} \alpha_1)^2}{\sigma_3^2 + N [2\sigma_{12}^2 (1 + \alpha_2) - \frac{\pi^2}{4} \alpha_1^2 \sigma_{12}^2]} \quad (5.95)$$

5.3.5 Mean of $\|\tilde{\mathbf{w}}\|^2$

The mean value of the total fading coefficient can be written as

$$\mu_{\|\tilde{\mathbf{w}}\|^2} = E [\|\tilde{\mathbf{w}}\|^2] = E \left[\sum_{k=1}^M |\tilde{w}_k|^2 \right]. \quad (5.96)$$

Since the fading coefficients are identically distributed, then

$$\mu_{\|\tilde{\mathbf{w}}\|^2} = M E[|\tilde{w}_k|^2], \quad (5.97)$$

and

$$\mu_{\|\tilde{\mathbf{w}}\|^2} = 4NM(1 + \alpha_2)\sigma_{12}^2 + 2M\sigma_3^2 \quad (5.98)$$

5.3.6 Variance of $\|\tilde{\mathbf{w}}\|^2$

The variance of the total fading coefficient is given as

$$\text{var}(\|\tilde{\mathbf{w}}\|^2) = \text{var}\left(\sum_{k=1}^M |\tilde{w}_k|^2\right). \quad (5.99)$$

Let $\tilde{Z}_k = |\tilde{w}_k|^2$, therefore

$$\text{var}(\|\tilde{\mathbf{w}}\|^2) = \text{var}\left(\sum_{i=1}^M \tilde{Z}_i\right) = M \times \text{var}(\tilde{Z}_i) + M(M-1) \times \text{cov}(\tilde{Z}_i, \tilde{Z}_k), \quad (5.100)$$

Since

$$\text{cov}(\tilde{Z}_i, \tilde{Z}_k) = E[\tilde{Z}_i \tilde{Z}_k] - E[\tilde{Z}_i] E[\tilde{Z}_k], \quad (5.101)$$

the expected value of the product of the squared magnitude of two different fading coefficients is

$$E[\tilde{Z}_i \tilde{Z}_k] = E[\tilde{c}_i^2 \tilde{c}_k^2] + 2E[\tilde{c}_i^2 \tilde{s}_k^2] + E[\tilde{s}_i^2 \tilde{s}_k^2] \quad (5.102)$$

The term $E[\tilde{c}_i^2 \tilde{c}_k^2]$ can be calculated by (5.103)

$$E[\tilde{c}_i^2 \tilde{c}_k^2] = \begin{cases} 2k_5 (\sigma_3^2 + k_6 - k_5 a_3) + (\sigma_3^2 + k_6 - k_5 a_3)^2 + \\ \frac{8}{\pi} k_5^3 a_3 (N+1) - 3k_5^4 + \left(\frac{2}{\pi} k_5 a_3 (N+1) - k_5^2\right)^2 & i \neq k \\ k_5^4 + 6k_5^2 (\sigma_3^2 + k_6 - k_5 a_3) + 3(\sigma_3^2 + k_6 - k_5 a_3)^2 & i = k \end{cases} \quad (5.103)$$

where $k_5 = N \frac{\pi}{2} \sigma_{12} \alpha_1$, $k_6 = 2N \sigma_{12}^2 (1 + \alpha_2)$ and $a_3 = \frac{\pi}{2} \sigma_{12} \alpha_1$. Since $E[\tilde{s}_k] = 0$, thus the fourth order moment of the quadrature component is

$$E[\tilde{s}_k^4] = 3(\text{var}(\tilde{s}_k))^2 = 3(N(2\sigma_{12}^2(1 - \alpha_2)) + \sigma_3^2)^2 = 3(k_7 + \sigma_3^2)^2 \quad (5.104)$$

where $k_7 = 2N \sigma_{12}^2 (1 - \alpha_2)$.

We need to obtain the term $E[\tilde{c}_i^2 \tilde{s}_k^2]$ without considering the CLT, because the correlation coefficient between \tilde{c} and \tilde{s} is zero. But the terms \tilde{c}_i^2 and \tilde{s}_k^2 are not independent and the approach that use the integral of the product to obtain the expected value is hard to solve analytically.

Considering the definition, we have that

$$E [\tilde{c}_i^2 \tilde{s}_k^2] = E \left[\left(\sum_{l=1}^N |g_{il}| |h_l^{LIS}| \cos \delta_{il} + \tilde{C}_{BS,i} \right)^2 \times \left(\sum_{m=1}^N |g_{km}| |h_m^{LIS}| \sin \delta_{km} + \tilde{S}_{BS,k} \right)^2 \right] \quad (5.105)$$

Expanding the power and the product of the two terms we can find the expression (5.106). Considering that $E [\tilde{C}_{BS,i}] = 0$, $E [\tilde{S}_{BS,k}] = 0$, $E [\tilde{S}_{BS,k}^2] = E [\tilde{S}_{BS,k}^2] = \sigma_3^2$ so (5.106) simplifies to (5.107). The three summation terms of (5.107) are obtained by (5.108), (5.109) and (5.110) that can be obtained by analyzing the different possible values of the summation indexes that can made the indexed terms dependents or independents.

$$\begin{aligned} E [\tilde{c}_i^2 \tilde{s}_k^2] = & E \left[\left(\sum_{l=1}^N |g_{il}| |h_l^{LIS}| \cos \delta_{il} \right)^2 \left(\sum_{m=1}^N |g_{km}| |h_m^{LIS}| \sin \delta_{km} \right)^2 \right] + E \left[\left(\sum_{l=1}^N |g_{il}| |h_l^{LIS}| \cos \delta_{il} \right)^2 \tilde{S}_{BS,k}^2 \right] + \\ & 2E \left[\left(\sum_{l=1}^N |g_{il}| |h_l^{LIS}| \cos \delta_{il} \right)^2 \left(\sum_{m=1}^N |g_{km}| |h_m^{LIS}| \sin \delta_{km} \right) \tilde{S}_{BS,k} \right] + 2E \left[\left(\sum_{l=1}^N |g_{il}| |h_l^{LIS}| \cos \delta_{il} \right) \tilde{C}_{BS,i} \tilde{S}_{BS,k}^2 \right] + \\ & + 2E \left[\left(\sum_{l=1}^N |g_{il}| |h_l^{LIS}| \cos \delta_{il} \right) \tilde{C}_{BS,i} \left(\sum_{m=1}^N |g_{km}| |h_m^{LIS}| \sin \delta_{km} \right)^2 \right] + E \left[\tilde{C}_{BS,i}^2 \left(\sum_{m=1}^N |g_{km}| |h_m^{LIS}| \sin \delta_{km} \right)^2 \right] + \\ & 4E \left[\left(\sum_{l=1}^N |g_{il}| |h_l^{LIS}| \cos \delta_{il} \right) \tilde{C}_{BS,i} \left(\sum_{m=1}^N |g_{km}| |h_m^{LIS}| \sin \delta_{km} \right) \tilde{S}_{BS,k} \right] + E [\tilde{C}_{BS,i}^2 \tilde{S}_{BS,k}^2] + \\ & 2E \left[\tilde{C}_{BS,i}^2 \left(\sum_{m=1}^N |g_{km}| |h_m^{LIS}| \sin \delta_{km} \right) \tilde{S}_{BS,k} \right] \quad (5.106) \end{aligned}$$

$$\begin{aligned} E [\tilde{c}_i^2 \tilde{s}_k^2] = & E \left[\left(\sum_{l=1}^N |g_{il}| |h_l^{LIS}| \cos \delta_{il} \right)^2 \left(\sum_{m=1}^N |g_{km}| |h_m^{LIS}| \sin \delta_{km} \right)^2 \right] \dots \\ & + E \left[\left(\sum_{l=1}^N |g_{il}| |h_l^{LIS}| \cos \delta_{il} \right)^2 \right] \sigma_3^2 + E \left[\left(\sum_{m=1}^N |g_{km}| |h_m^{LIS}| \sin \delta_{km} \right)^2 \right] \sigma_3^2 + \sigma_3^4 \quad (5.107) \end{aligned}$$

$$\begin{aligned} E \left[\left(\sum_{l=1}^N |g_{il}| |h_l^{LIS}| \cos \delta_{il} \right)^2 \right] = & E \left[\sum_{l=1}^N \sum_{t=1}^N |g_{il}| |g_{it}| |h_l^{LIS}| |h_t^{LIS}| \cos \delta_{il} \cos \delta_{it} \right] = \\ & 2N \sigma_{12}^2 (1 + \alpha_2) + (N^2 - N) \left(\frac{\pi}{2} \right)^2 \sigma_{12}^2 \alpha_1^2 \quad (5.108) \end{aligned}$$

$$E \left[\left(\sum_{m=1}^N |g_{km}| |h_m^{LIS}| \sin \delta_{km} \right)^2 \right] = E \left[\sum_{d=1}^N \sum_{m=1}^N |g_{kd}| |g_{km}| |h_d^{LIS}| |h_m^{LIS}| \sin \delta_{kd} \sin \delta_{km} \right] =$$

$$2N\sigma_{12}^2(1 - \alpha_2) \quad (5.109)$$

$$E \left[\left(\sum_{l=1}^N |g_{il}| |h_l^{LIS}| \cos \delta_{il} \right)^2 \left(\sum_{m=1}^N |g_{km}| |h_m^{LIS}| \sin \delta_{km} \right)^2 \right] =$$

$$E \left[\sum_{l=1}^N \sum_{t=1}^N \sum_{d=1}^N \sum_{m=1}^N |g_{il}| |g_{it}| |g_{kd}| |g_{km}| |h_l^{LIS}| |h_t^{LIS}| |h_d^{LIS}| |h_m^{LIS}| \cos \delta_{il} \cos \delta_{it} \sin \delta_{kd} \sin \delta_{km} \right] \quad (5.110)$$

$$E [\tilde{c}_i^2 \tilde{s}_k^2] = \begin{cases} (N-1)k_{10} + 3(N^2 - N)k_9 + 2k_{10} + (N^3 - 3N^2 + 2N)k_9 \dots \\ + \left(k_6 + \frac{(N-1)}{N}k_5 + k_7 \right) \sigma_3^2 + \sigma_3^4 & i \neq k \\ (N-1)k_8 + \frac{9}{2}(N^2 - N)k_{11} + 4k_{10} + (N^3 - 3N^2 + 2N)k_9 \dots \\ + \left(k_6 + \frac{(N-1)}{N}k_5 + k_7 \right) \sigma_3^2 + \sigma_3^4 & i = k \end{cases}$$

where

$$k_8 = 2N\sigma_{12}^4(1 - \alpha_4), \quad k_9 = 2 \left(\frac{\pi}{2} \right)^2 \sigma_{12}^4 \alpha_1^2 (1 - \alpha_2), \quad k_{10} = 4N\sigma_{12}^4(1 - \alpha_2^2), \quad k_{11} =$$

$$\left(\frac{\pi}{2} \right)^2 \sigma_{12}^4 \alpha_1 (\alpha_1 - \alpha_3) \quad (5.111)$$

$$E[\tilde{Z}_i \tilde{Z}_k] =$$

$$\begin{cases} 2k_5 (\sigma_3^2 + k_6 - k_5 a_3) + (\sigma_3^2 + k_6 - k_5 a_3)^2 + \frac{8}{\pi} k_5^3 a_3 (N+1) - 3k_5^4 + \left(\frac{2}{\pi} k_5 a_3 (N+1) - k_5^2 \right)^2 + \\ 2 \left[(N-1)k_{10} + 3(N^2 - N)k_9 + 2k_{10} + (N^3 - 3N^2 + 2N)k_9 + \left(k_6 + \frac{(N-1)}{N}k_5 + k_7 \right) \sigma_3^2 + \sigma_3^4 \right] + \\ 2(\sigma_3^2 + k_6 - k_5 a_3 + k_5^2) (k_7 + \sigma_3^2) + (k_7 + \sigma_3^2)^2 & i \neq k \\ k_5^4 + 6k_5^2 (\sigma_3^2 + k_6 - k_5 a_3) + 3(\sigma_3^2 + k_6 - k_5 a_3)^2 + 2(\sigma_3^2 + k_6 - k_5 a_3 + k_5^2) (k_7 + \sigma_3^2) + \\ 2 \left[(N-1)k_8 + \frac{9}{2}(N^2 - N)k_{11} + 4k_{10} + (N^3 - 3N^2 + 2N)k_9 + \left(k_6 + \frac{(N-1)}{N}k_5 + k_7 \right) \sigma_3^2 + \sigma_3^4 \right] + \\ 3(k_7 + \sigma_3^2)^2 & i = k \end{cases}$$

$$(5.112)$$

Thus the covariance $\text{cov}(\tilde{Z}_i, \tilde{Z}_k)$ can be obtained by (5.101), where $E[\tilde{Z}_i \tilde{Z}_k]$ is given by (5.112), remember that $E[\tilde{Z}_i] = E[\tilde{Z}_k]$ and $E[\tilde{Z}_k] = E[|\tilde{w}_k|^2]$ that can be calculated by (5.89), also consider that $\text{var}(\tilde{Z}_k) = \text{cov}(\tilde{Z}_k, \tilde{Z}_k)$ and the variance of the overall fading coefficient is given by (5.113).

$$\begin{aligned} \sigma_{\|\tilde{\mathbf{w}}\|^2}^2 &= \text{var}(\|\tilde{\mathbf{w}}\|^2) = \\ &M(M-1) \left[2k_5(\sigma_3^2 + k_6 - k_5 a_3) + (\sigma_3^2 + k_6 - k_5 a_3)^2 + \frac{8}{\pi} k_5^3 a_3 (N+1) - 3k_5^4 + \left(\frac{2}{\pi} k_5 a_3 (N+1) - k_5^2 \right)^2 + \right. \\ &2 \left((N-1)k_{10} + 3(N^2 - N)k_9 + 2k_{10} + (N^3 - 3N^2 + 2N)k_9 + \left(k_6 + \frac{(N-1)}{N} k_5 + k_7 \right) \sigma_3^2 + \sigma_3^4 \right) + \\ &\quad \left. 2(\sigma_3^2 + k_6 - k_5 a_3 + k_5^2)(k_7 + \sigma_3^2) + (k_7 + \sigma_3^2)^2 - (2k_6 + 2\sigma_3^2)^2 \right] + \\ &M \left[k_5^4 + 6k_5^2(\sigma_3^2 + k_6 - k_5 a_3) + 3(\sigma_3^2 + k_6 - k_5 a_3)^2 + 2(\sigma_3^2 + k_6 - k_5 a_3 + k_5^2)(k_7 + \sigma_3^2) + \right. \\ &2 \left((N-1)k_8 + \frac{9}{2}(N^2 - N)k_{11} + 4k_{10} + (N^3 - 3N^2 + 2N)k_9 + \left(k_6 + \frac{(N-1)}{N} k_5 + k_7 \right) \sigma_3^2 + \sigma_3^4 \right) + \\ &\quad \left. 3(k_7 + \sigma_3^2)^2 - (2k_6 + 2\sigma_3^2)^2 \right] \quad (5.113) \end{aligned}$$

5.4 Trigonometric Moments of a Von Mises Random Variable

Since the Von Mises distribution is symmetric about zero, therefore the expected values of odd functions applied to a Von Mises distributed random variable will be zero, therefore

$$\forall n, m \in \mathbb{Z} \quad E[\sin^{2n+1} \delta \cos^m \delta] = 0, \quad (5.114)$$

on the other hand, the expected value of a power of even trigonometric functions must be expanded in trigonometric Fourier series, or simply transformed in a superposition of cosine and sine functions using trigonometric transformations to allow us to use the characteristic function definition.

Since $E[\cos p\delta] = \alpha_p$, we have that

$$E[\cos^2 \delta] = E\left[\frac{1}{2}(1 + \cos 2\delta)\right] = \frac{1}{2}(1 + \alpha_2), \quad (5.115)$$

$$E[\cos^3 \delta] = E\left[\frac{1}{4}(3 \cos \delta + \cos 3\delta)\right] = \frac{1}{4}(3\alpha_1 + \alpha_3), \quad (5.116)$$

and

$$E[\cos^4 \delta] = E \left[\frac{1}{8} (3 + 4 \cos 2\delta + \cos 4\delta) \right] = \frac{1}{8} (3 + 4\alpha_2 + \alpha_4). \quad (5.117)$$

We can write the power of a sine function in terms of the cosine function by applying the algebraic transformation $\sin^2 \delta = 1 - \cos^2 \delta$, and this substitution is useful only when the power is even. The expected value is zero for every odd power of $\sin \delta$.

References

- 1 COELHO FERREIRA, R. et al. Large Intelligent Surfaces Communicating Through Massive MIMO Rayleigh Fading Channels. **Sensors**, Multidisciplinary Digital Publishing Institute, v. 20, n. 22, p. 6679, 2020.
- 2 FERREIRA, R. C. et al. Bit Error Probability for Large Intelligent Surfaces Under Double-Nakagami Fading Channels. **IEEE Open Journal of the Communications Society**, IEEE, 2020.
- 3 ZHANG, Z. et al. 6G wireless networks: Vision, requirements, architecture, and key technologies. **IEEE Vehicular Technology Magazine**, IEEE, v. 14, n. 3, p. 28–41, 2019.
- 4 FERNANDO, X.; FARAHNEH, H. **Visible Light Communications**. [S.l.]: IOP Publishing, 2019. (2053-2563). ISBN 978-0-7503-2284-3. DOI: [10.1088/978-0-7503-2284-3](https://doi.org/10.1088/978-0-7503-2284-3).
- 5 NAWAZ, S. J. et al. Quantum machine learning for 6G communication networks: State-of-the-art and vision for the future. **IEEE Access**, IEEE, v. 7, p. 46317–46350, 2019.
- 6 YU, X.; XU, D.; SCHOBBER, R. MISO wireless communication systems via intelligent reflecting surfaces. In: IEEE International Conference on Communications in China. [S.l.: s.n.], 2019. P. 735–740.
- 7 ZHAO, J.; LIU, Y. A Survey of Intelligent Reflecting Surfaces (IRSs): Towards 6G Wireless Communication Networks. **arXiv preprint arXiv:1907.04789**, 2019.
- 8 BASAR, E. et al. Wireless communications through reconfigurable intelligent surfaces. **IEEE Access**, IEEE, v. 7, p. 116753–116773, 2019.
- 9 HE, Z.-Q.; YUAN, X. Cascaded channel estimation for large intelligent metasurface assisted massive MIMO. **IEEE Wireless Communications Letters**, IEEE, 2019.
- 10 BASAR, E. Large intelligent surface-based index modulation: A new beyond MIMO paradigm for 6G. **arXiv preprint arXiv:1904.06704**, 2019.

- 11 MISHRA, D.; JOHANSSON, H. Channel estimation and low-complexity beamforming design for passive intelligent surface assisted MISO wireless energy transfer. In: IEEE International Conference on Acoustics, Speech and Signal Processing. [S.l.: s.n.], 2019. P. 4659–4663.
- 12 WU, Q.; ZHANG, R. Intelligent reflecting surface enhanced wireless network via joint active and passive beamforming. **IEEE Transactions on Wireless Communications**, IEEE, v. 18, n. 11, p. 5394–5409, 2019.
- 13 VITTURI, S.; ZUNINO, C.; SAUTER, T. Industrial Communication Systems and Their Future Challenges: Next-Generation Ethernet, IoT, and 5G. **Proceedings of the IEEE**, v. 107, n. 6, p. 944–961, June 2019. ISSN 1558-2256. DOI: [10.1109/JPROC.2019.2913443](https://doi.org/10.1109/JPROC.2019.2913443).
- 14 PUGLIELLI, A. et al. A scalable massive MIMO array architecture based on common modules. In: INTERNATIONAL Conference on Communication Workshop (ICCW). [S.l.: s.n.], June 2015. DOI: [10.1109/ICCW.2015.7247359](https://doi.org/10.1109/ICCW.2015.7247359).
- 15 WANG, Z.; LIU, L.; CUI, S. Channel Estimation for Intelligent Reflecting Surface Assisted Multiuser Communications. In: 2020 IEEE Wireless Communications and Networking Conference (WCNC). [S.l.: s.n.], 2020. P. 1–6.
- 16 TATARIA, H.; TUFVESSON, F.; EDFORS, O. Real-Time Implementation Aspects of Large Intelligent Surfaces. In: ICASSP 2020 - 2020 IEEE International Conference on Acoustics, Speech and Signal Processing (ICASSP). [S.l.: s.n.], 2020. P. 9170–9174.
- 17 ELBIR, A. M. et al. Deep Channel Learning For Large Intelligent Surfaces Aided mm-Wave Massive MIMO Systems. **IEEE Wireless Communications Letters**, p. 1–1, 2020.
- 18 YU, G. et al. Design, Analysis and Optimization of A Large Intelligent Reflecting Surface Aided B5G Cellular Internet of Things. **IEEE Internet of Things Journal**, p. 1–1, 2020.
- 19 HUM, S. V.; PERRUISSEAU-CARRIER, J. Reconfigurable reflectarrays and array lenses for dynamic antenna beam control: A review. **IEEE Transactions on Antennas and Propagation**, IEEE, v. 62, n. 1, p. 183–198, 2013.

- 20 HU, S.; RUSEK, F.; EDFORS, O. Beyond massive MIMO: The potential of data transmission with large intelligent surfaces. **IEEE Transactions on Signal Processing**, IEEE, v. 66, n. 10, p. 2746–2758, 2018.
- 21 PEREIRA DE FIGUEIREDO, F. A. et al. On the application of massive mimo systems to machine type communications. eng. **IEEE Access**, Ieee-inst Electrical Electronics Engineers Inc, v. 7, p. 2589–2611, 2019. ISSN 2169-3536.
- 22 HUANG, C. et al. Reconfigurable intelligent surfaces for energy efficiency in wireless communication. **IEEE Transactions on Wireless Communications**, IEEE, v. 18, n. 8, p. 4157–4170, 2019.
- 23 YE, J.; GUO, S.; ALOUINI, M.-S. Joint reflecting and precoding designs for SER minimization in reconfigurable intelligent surfaces assisted MIMO systems. **arXiv preprint arXiv:1906.11466**, 2019.
- 24 BAO, W. et al. Joint Rate Control and Power Allocation for Non-Orthogonal Multiple Access Systems. **IEEE Journal on Selected Areas in Communications**, v. 35, n. 12, p. 2798–2811, Dec. 2017. ISSN 1558-0008. DOI: [10.1109/JSAC.2017.2726357](https://doi.org/10.1109/JSAC.2017.2726357).
- 25 RENZO, M. D. et al. **Smart Radio Environments Empowered by AI Reconfigurable Meta-Surfaces: An Idea Whose Time Has Come**. [S.l.: s.n.], 2019.
- 26 ZHANG, H. et al. Reconfigurable intelligent surfaces assisted communications with limited phase shifts: How many phase shifts are enough? **IEEE Transactions on Vehicular Technology**, IEEE, 2020.
- 27 HUANG, C. et al. Energy Efficient Multi-User MISO Communication using Low Resolution Large Intelligent Surfaces. **CoRR**, abs/1809.05397, 2018.
- 28 TAHA, A.; ALRABEIAH, M.; ALKHATEEB, A. **Deep learning for large intelligent surfaces in millimeter wave and massive MIMO systems**. [S.l.]: May, 2019.
- 29 PEROVIĆ, N. S.; DI RENZO, M.; FLANAGAN, M. F. Channel capacity optimization using reconfigurable intelligent surfaces in indoor mmWave environments. **arXiv preprint arXiv:1910.14310**, 2019.

- 30 NTONTIN, K. et al. Reconfigurable intelligent surfaces vs. relaying: Differences, similarities, and performance comparison. **arXiv preprint arXiv:1908.08747**, 2019.
- 31 YANG, Y. et al. Intelligent reflecting surface meets OFDM: Protocol design and rate maximization. **IEEE Transactions on Communications**, IEEE, 2020.
- 32 YE, J.; GUO, S.; ALOUINI, M. Joint Reflecting and Precoding Designs for SER Minimization in Reconfigurable Intelligent Surfaces Assisted MIMO Systems. **IEEE Transactions on Wireless Communications**, p. 1–1, 2020.
- 33 YUE, D.-W.; NGUYEN, H. H.; SUN, Y. **mmWave Doubly-Massive-MIMO Communications Enhanced with an Intelligent Reflecting Surface**. [S.l.: s.n.], 2020. arXiv: 2003.00282 [eess.SP].
- 34 HE, J. et al. Large Intelligent Surface for Positioning in Millimeter Wave MIMO Systems. In: 2020 IEEE 91st Vehicular Technology Conference (VTC2020-Spring). [S.l.: s.n.], 2020. P. 1–5.
- 35 DARDARI, D. Communicating with Large Intelligent Surfaces: Fundamental Limits and Models. **IEEE Journal on Selected Areas in Communications**, p. 1–1, 2020.
- 36 JUNG, M. et al. Performance Analysis of Large Intelligent Surfaces (LISs): Asymptotic Data Rate and Channel Hardening Effects. **IEEE Transactions on Wireless Communications**, v. 19, n. 3, p. 2052–2065, 2020.
- 37 YAN, W. et al. Passive Beamforming and Information Transfer Design for Reconfigurable Intelligent Surfaces Aided Multiuser MIMO Systems. **IEEE Journal on Selected Areas in Communications**, p. 1–1, 2020.
- 38 BADIU, M.; COON, J. P. Communication Through a Large Reflecting Surface With Phase Errors. **IEEE Wireless Communications Letters**, v. 9, n. 2, p. 184–188, 2020.
- 39 CAVERS, J. K. Single-user and multiuser adaptive maximal ratio transmission for Rayleigh channels. **IEEE Transactions on Vehicular Technology**, v. 49, n. 6, p. 2043–2050, 2000.
- 40 MAKARFI, A. U. et al. Physical Layer Security in Vehicular Networks with Reconfigurable Intelligent Surfaces. In: 2020 IEEE 91st Vehicular Technology Conference (VTC2020-Spring). [S.l.: s.n.], 2020. P. 1–6.

- 41 QIAN, X. et al. Beamforming Through Reconfigurable Intelligent Surfaces in Single-User MIMO Systems: SNR Distribution and Scaling Laws in the Presence of Channel Fading and Phase Noise. **arXiv preprint arXiv:2005.07472**, 2020.
- 42 BJÖRNSON, E.; SANGUINETTI, L. Rayleigh Fading Modeling and Channel Hardening for Reconfigurable Intelligent Surfaces. **arXiv preprint arXiv:2009.04723**, 2020.
- 43 KUDATHANTHIRIGE, D.; GUNASINGHE, D.; AMARASURIYA, G. Performance Analysis of Intelligent Reflective Surfaces for Wireless Communication. **arXiv preprint arXiv:2002.05603**, 2020.
- 44 SUZUKI, H. A Statistical Model for Urban Radio Propagation. **IEEE Transactions on Communications**, v. 25, n. 7, p. 673–680, 1977.
- 45 AULIN, T. Characteristics of a digital mobile radio channel. **IEEE Transactions on Vehicular Technology**, v. 30, n. 2, p. 45–53, 1981.
- 46 NAKAGAMI, M. The m -distribution—A general formula of intensity distribution of rapid fading. In: **STATISTICAL methods in radio wave propagation**. [S.l.]: Elsevier, 1960. P. 3–36.
- 47 GONG, S. et al. Toward Smart Wireless Communications via Intelligent Reflecting Surfaces: A Contemporary Survey. **IEEE Communications Surveys & Tutorials**, IEEE, v. 22, n. 4, p. 2283–2314, 2020.
- 48 BADIU, M.-A.; COON, J. P. Communication through a large reflecting surface with phase errors. **IEEE Wireless Communications Letters**, IEEE, v. 9, n. 2, p. 184–188, 2019.
- 49 ABRAMOWITZ, M.; STEGUN, I. A. **Handbook of Mathematical Functions with Formulas, Graphs, and Mathematical Tables**. 10th edition. New York: Dover, 1964.
- 50 MAGHSOODI, Y. Exact distributions of envelopes of sums of stochastic sinusoids with general random amplitudes and phases. **Scinance Analytics**, 2004.
- 51 ROSENBLATT, M. A central limit theorem and a strong mixing condition. **Proceedings of the National Academy of Sciences of the United States of America**, National Academy of Sciences, v. 42, n. 1, p. 43, 1956.

- 52 PAPOULIS, A.; PILLAI, S. U. **Probability, Random Variables, and Stochastic Processes**. Fourth. Boston: McGraw Hill, 2002. ISBN 0071122567 9780071122566 0073660116 9780073660110 0071226613 9780071226615.
- 53 PROAKIS. **Digital Communications 5th Edition**. [S.l.]: McGraw Hill, 2007.
- 54 CARRILLO, D. et al. Bit error probability for MMSE receiver in GFDM systems. **IEEE Communications Letters**, IEEE, v. 22, n. 5, p. 942–945, 2018.
- 55 MARY, P. et al. BPSK Bit Error Outage over Nakagami-m Fading Channels in Lognormal Shadowing Environments. **IEEE Communications Letters**, v. 11, p. 565–567, Aug. 2007. DOI: [10.1109/LCOMM.2007.070241](https://doi.org/10.1109/LCOMM.2007.070241).
- 56 NADEEM, Q.-U.-A. et al. Asymptotic Analysis of Large Intelligent Surface Assisted MIMO Communication. **ArXiv**, abs/1903.08127, 2019.
- 57 COVER, T. M.; THOMAS, J. A. **Elements of Information Theory (Wiley Series in Telecommunications and Signal Processing)**. USA: Wiley-Interscience, 2006. ISBN 0471241954.
- 58 GOLDSMITH, A. **Wireless communications**. [S.l.]: Cambridge university press, 2005.